

Supporting Information

Construction of highly fluorescent N-O seven-membered heterocycles via thermo-oxidation of oxazolidines

Qiaonan Chen,^a Xiao Liang,^c Jiahui Du,^a Zhonglin Wei,^b Yu-Mo Zhang,^b Ting Zhang,^a Tianyou Qin,^b Wenbin Gao,^b Lan Sheng,^{*b} and Sean Xiao-An Zhang^{*a,b}

^a State Key Laboratory of Supramolecular Structure and Materials, College of Chemistry,
Jilin University, Changchun, 130012, P. R. China

E-mail: seanzhang@jlu.edu.cn; Fax: +86-431-85153812

^b College of Chemistry, Jilin University, Changchun, 130012, P. R. China

E-mail: shenglan17@jlu.edu.cn; Fax: +86-431-85153812

^c Key Laboratory for Molecular Enzymology and Engineering of Ministry of
Education, School of Life Sciences, Jilin University, Changchun, 130012, P. R. China

Table of Contents

1. General experimental information.....	S4
2. Synthesis of 2a-2f, I and 3.....	S6
3. ^1H NMR spectra monitoring heating 1a-1f in DMSO- d_6	S11
4. Structural characterizations of intermediate product I of 1b reacting with CH ₃ I.....	S12
5. ^1H NMR spectra monitoring heating I in DMSO- d_6	S13
6. Photographs of heating CH ₃ I in DMSO.....	S14
7. HRMS spectra and ^1H NMR spectra monitoring reaction of 1g and CH ₃ I in DMF and DMSO- d_6 at 120 °C.....	S15
8. ^1H NMR spectra monitoring heating 1b-OF in DMSO- d_6	S16
9. Comparison of 1b-OF reaction in DMSO under aerobic and anaerobic conditions.....	S18
10. Reaction of 1a-OF with H ₂ O ₂ in DMF.....	S19
11. Reaction of 1b-OF in DMSO/DMF with addition of radical inhibitor BHT....	S20
12. HRMS spectra for reaction solutions of 1b with NIS, NBS and NCS.....	S21
13. Crystal data and structure refinement for 2a, 2b, 2c and 3.....	S22
14. Spectral data of 1a-OF-1f-OF and 2a-2f in DCM solutions and PMMA films.....	S24
15. Fluorescent photographs of solid powders of 1a-OF-1f-OF, 2a-2f.....	S28
16. Solvent polarity effects on optical properties of 2a-2f.....	S29
17. Photographs, UV-Vis spectra and fluorescent spectra of 2a-2f in PMMA with different weight percent.....	S32
18. Comparison of fluorescence quantum efficiency of 2a and 2c with I ⁻ , Br ⁻ and PF ₆ ⁻	S34

19. Theoretical calculations of 2a-2f.....	S36
20. Photostability and thermal stability of 2a-2f.....	S37
21. HRMS spectra of 2b-OH and UV-Vis spectra measurement for switch property of 2b.....	S39
22. Measurement of the pKa' of 2a-2f.....	S40
23. HRMS spectra monitoring reaction of 2b and amines.....	S41
24. The selectivity to pH of 2b over reactive nitrogen and oxygen species.....	S42
25. The cytotoxicity of 2e.....	S43
26. Effect of extracellular fluctuations under oxidative stress and with drug treatment on endocytosis efficiency and fluorescence of 2e.....	S44
27. ^1H NMR and ^{13}C NMR spectra.....	S45
28. The coordination of structures.....	S53
29. References.....	S62

1. General experimental information

Materials

Phenylhydrazine (98 %), 4-nitrophenylhydrazine (98 %), 4-methoxyphenylhydrazine hydrochloride (98 %), 4-dimethylaminobenzaldehyde (99 %) and diethyl malonate (99 %) were purchased from Sinopharm Chemical Reagent Co., Ltd. (Beijing, China). 3-Methyl-2-butanone (98 %), 2-bromoethanol (98 %), anisic aldehyde (99 %), 4-(Diethylamino)salicylaldehyde (98 %), Iodomethane (99.5 %), Iodine (98 %) and *N*-iodosuccinimide (98 %) were purchased from Energy Chemical (Shanghai, China). Sodium chloride (NaCl), sodium carbonate (Na₂CO₃) and anhydrous sodium sulfate (Na₂SO₄) were purchased from Beijing Chemical Factory (Beijing, China). Lysotracker Green and CellLight™ Mitochondria-GFP were obtained from Thermo Fisher (Eugene, OR). 4,6-diamidino-2-phenylindole (DAPI) were obtained from Amersham (Solon, USA). Solvents: Dimethyl sulfoxide (DMSO, HPLC) was purchased from Tianjin Guangfu Fine Chemical Research Institute (Tianjin, China); dimethylformamide (DMF) from Beijing Chemical Factory (Beijing, China). Unless otherwise stated, all reagents and solvents were used without further purification.

Instruments

The UV-Vis absorption spectra were measured using a 0.1 cm quartz cuvette on a Shimadzu UV-2550 PC double-beam spectrophotometer. The fluorescent emission spectra were measured using a 0.1 cm quartz cuvette on a Shimadzu RF-5301 PC spectrofluorophotometer with a xenon lamp as a light source. The fluorescence quantum yields (Φ_f) and fluorescence lifetime (under the excitation at 400 nm) were measured on Edinburgh FLS 920 steady state spectrometer. The LC-HRMS (ESI) analysis was performed on an Agilent 1290-micro TOF-Q II mass spectrometer. ¹H NMR and ¹³C NMR spectra were recorded on a Bruker AVANCE500 (500M) and Wuhan Zhongke Niujin As 400 (400M) at room temperature and were reported in ppm and determined with tetramethylsilane (TMS) or respect to residual signals of the deuterated solvents as internal standards (TMS, 0.00; CDCl₃, 7.26; DMSO-*d*₆, 2.50 for ¹H NMR and CDCl₃, 77.0; DMSO-*d*₆, 39.5 for ¹³C NMR). Melting point was determined using a SGW X-4B microscopy melting point apparatus. Flow cytometry (cyto FLEX, Beckman COULTER). Confocal laser scanning microscope (Carl Zeiss Microscopy LLC, Jena, Germany).

Methods

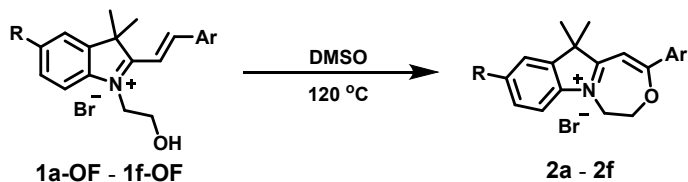
Cytotoxicity assays. The viabilities of cells treated with **2e** were measured by a well-established 3-(4, 5-dimethylthiazol-2-yl)-2, 5-diphenyltetrazolium bromide (MTT) assay. Generally, HeLa cells, A549 cells and SW480 cells were seeded in 96-well plates harboring 2 mL of 10% FBS-containing DMEM at a density of 8000 cells per well. The cells were incubated with drugs at concentrations from 0 to 100 $\mu\text{g}/\text{mL}$, and cells without treatment were used as a control. After the incubation at 37 °C for 20 h, the standard MTT assay was used to determine the cell viability. Five repeats were conducted for each sample.

Co-localization experiments of **2e with commercial organelle-specific probes.** HeLa cells were seeded into 6-well plates at a density of 2.5×10^5 cells/well and cultured with a sterilized coverslip for 12 h. Then the cells were treated with **2e** at the concentration of 1 $\mu\text{g}/\text{mL}$ for 4 h, respectively. Afterwards, the cells were stained with CellLight™ Mitochondria-GFP and Lysotracker Green DND-26 according to the manufacturer's protocol, respectively. Then the cells were washed with PBS for three times, followed by fixing with cold 75% ethanol at 4 °C for 20 min and then stained with DAPI solution. Finally, the cover slips were taken from the wells and observed with confocal laser scanning microscope (CLSM).

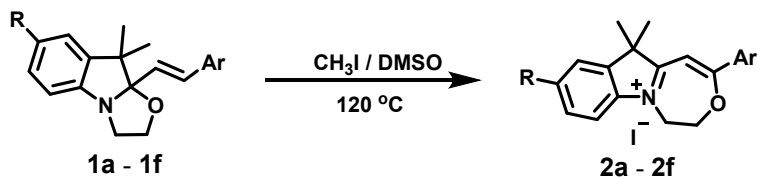
Visualizing extracellular fluctuations under oxidative stress and with drug treatment. Rosup, 5-fluorouracil (5-FU) and methotrexate (MTX) were used to construct oxidative and drug environments and then the endocytosis of **2e** was detected under these conditions. HeLa cells were seed into 6-well plates at a density of 2.5×10^5 cells/well, and first, the cells were treated with Rosup, 5-FU and MTX, respectively. Then the medium was discarded after 1 hour treatment, and the cells were washed with phosphate buffer saline (PBS) three times. After that, **2e** was incubated with cells at concentration of 1 $\mu\text{g}/\text{mL}$ for 4 h. The endocytosis efficiency of **2e** was determined by flow cytometry and CLSM.

2. Synthesis of **2a-2f**, **I** and **3**

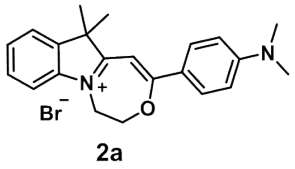
2.1 Synthesis of thermo-oxidation products oxazolidines (**2a-2f**)



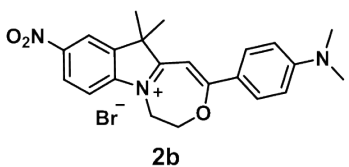
General synthesis method 1 of **2a-2f**. Starting materials **1a-OF-1f-OF** were prepared as reported.^{S1} **1a-OF-1f-OF** (100 mg) was stirred in dimethyl sulphoxide (2 mL) at 120 °C for 2 ~ 11 h (for **1f-OF**, 10 mg I₂ was added to prevent ring-closing of it). The reaction mixture was added with saturated solution of NaCl (20 mL). Dichloromethane (CH₂Cl₂) was added to extract product for 2 times and the CH₂Cl₂ layer was washed with saturated solution of NaCl for 1 time. Then the solvent was dried with anhydrous sodium sulfate and removed under reduced pressure. The crude mixture was precipitated as black solid. Purification of the crude mixture by chromatography (CH₂Cl₂ / MeOH = 50 / 1 to 20 / 1) afforded the product **2a-2f**. The products for characterizations below were obtained by method 1.



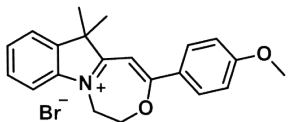
General synthesis method 2 of **2a-2f**. Starting materials **1a-1f** were prepared as reported.^{S1} A mixture of **1s** (0.37 mmol) and iodomethane (8 mmol) was stirred in dimethyl sulphoxide (2 mL) at 120 °C for 11 h. The reaction mixture was precipitated by addition of saturated solution of NaCl (20 mL) and filtered as brown powder. Purification of the crude reaction mixture by chromatography (CH₂Cl₂ / MeOH = 50 / 1 to 20 / 1) afforded the product **2a-2f**.



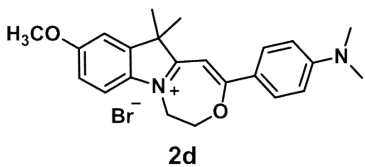
Yield: 31 %. m.p. 239.5 – 240.5 °C; ¹H NMR (500 MHz, DMSO-*d*₆): δ 8.03 (d, *J* = 9.2 Hz, 2H), 7.69 (d, *J* = 7.4 Hz, 1H), 7.58 (d, *J* = 7.4 Hz, 1H), 7.51 (t, *J* = 7.4 Hz, 1H), 7.41 (t, *J* = 7.4 Hz, 1H), 6.85 (d, *J* = 9.2 Hz, 2H), 6.59 (s, 1H), 5.02 (s, 2H), 4.65 (s, 2H), 3.12 (s, 6H), 1.62 (s, 6H); ¹³C NMR (126 MHz, DMSO-*d*₆): δ 176.9, 176.5, 154.1, 142.3, 139.9, 131.1, 128.5, 126.4, 123.1, 117.9, 112.2, 111.5, 85.8, 70.2, 51.2, 49.0, 24.7; LC-HRMS (ESI): m/z calculated for [M + H]⁺ 333.1961, found 333.1967.



Yield: 28 %. m.p. 246.9 – 247.9 °C; ¹H NMR (400 MHz, DMSO-*d*₆): δ 8.62 (s, 1H), 8.43 (d, *J* = 8.7 Hz, 1H), 8.08 (d, *J* = 8.7 Hz, 2H), 7.73 (d, *J* = 8.7 Hz, 1H), 6.89 (d, *J* = 8.7 Hz, 2H), 6.68 (s, 1H), 5.07 (s, 2H), 4.66 (s, 2H), 3.16 (s, 6H), 1.68 (s, 6H); ¹³C NMR (100 MHz, DMSO-*d*₆): δ 178.3, 178.0, 154.9, 147.4, 145.2, 140.9, 132.1, 125.3, 118.9, 117.4, 112.4, 111.8, 86.9, 70.6, 50.9, 49.3, 39.77, 24.8; LC-HRMS (ESI): m/z calculated for [M + H]⁺ 378.1812, found 378.1815.

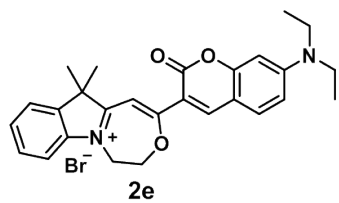


Yield: 30 %. m.p. 229.8 – 230.7 °C; ¹H NMR (500 MHz, DMSO-*d*₆): δ 8.15 (d, *J* = 8.9 Hz, 2H), 7.74 (d, *J* = 8.0 Hz, 1H), 7.69 (d, *J* = 8.0 Hz, 1H), 7.56 (t, *J* = 7.5 Hz, 1H), 7.48 (t, *J* = 7.5 Hz, 1H), 7.17 (d, *J* = 8.9 Hz, 2H), 6.78 (s, 1H), 5.10 (s, 2H), 4.77 (s, 2H), 3.90 (s, 3H), 1.65 (s, 6H); ¹³C NMR (100 MHz, DMSO-*d*₆): δ 178.9, 176.0, 164.0, 142.1, 140.4, 131.1, 128.6, 127.3, 124.7, 123.2, 114.6, 113.1, 88.0, 70.7, 55.9, 51.9, 49.5, 24.0. LC-HRMS (ESI): m/z calculated for [M + H]⁺ 320.1645, found 320.1644.

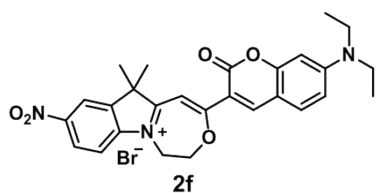


Yield: 30 %. m.p. 225.1 – 226.0 °C; ¹H NMR (400 MHz, DMSO-*d*₆): δ 7.99 (d, *J* = 9.1 Hz, 2H), 7.51 (d, *J* = 8.7 Hz, 1H), 7.35 (d, *J* = 2.3 Hz, 1H), 7.06 (dd, *J* = 8.7, 2.3 Hz, 1H), 6.84 (d, *J* = 9.1 Hz, 2H), 6.53 (s, 1H), 4.98 (s, 2H), 4.63 (s, 2H), 3.83 (s, 3H), 3.11 (s, 6H), 1.61 (s, 6H); ¹³C NMR (126 MHz, DMSO-*d*₆): δ 175.9, 175.4, 158.8, 153.9, 141.9, 135.8, 130.8, 118.1, 113.5, 113.3, 111.5, 109.5, 85.7,

70.0, 55.9, 51.3, 49.3, 24.6. LC-HRMS (ESI): m/z calculated for $[M + H]^+$ 363.2067, found 363.2073.

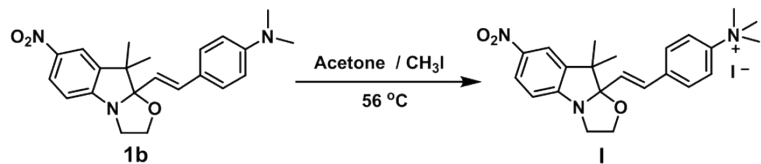


Yield: 29 %. m.p. 214.3 – 215.2 °C; ^1H NMR (400 MHz, DMSO- d_6): δ 8.70 (s, 1H), 7.75 (d, $J = 7.2$ Hz, 1H), 7.72 (d, $J = 9.1$ Hz, 1H), 7.66 (d, $J = 8.0$ Hz, 1H), 7.56 (t, $J = 7.4$ Hz, 1H), 7.47 (t, $J = 7.4$ Hz, 1H), 7.38 (s, 1H), 6.92 (d, $J = 9.1$ Hz, 1H), 6.69 (s, 1H), 5.03 (s, 2H), 4.73 (s, 2H), 3.56 (q, $J = 7.0$ Hz, 4H), 1.57 (s, 6H), 1.17 (t, $J = 7.0$ Hz, 6H); ^{13}C NMR (100 MHz, DMSO- d_6): δ 177.9, 171.3, 158.7, 158.0, 154.1, 147.3, 142.4, 140.0, 132.8, 128.7, 127.2, 123.3, 113.0, 111.2, 108.7, 108.0, 96.0, 90.5, 70.1, 51.3, 49.7, 44.8, 24.7, 12.4. LC-HRMS (ESI): m/z calculated for $[M + H]^+$ 429.2173, found 429.2174.



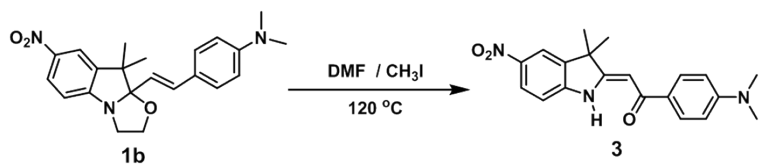
Yield: 16 %. m.p. 174.5 – 175.2 °C; ^1H NMR (400 MHz, DMSO- d_6): δ 8.74 (s, 1H), 8.71 (d, $J = 2.3$ Hz, 1H), 8.45 (dd, $J = 8.8, 2.3$ Hz, 1H), 7.84 (d, $J = 8.8$ Hz, 1H), 7.75 (d, $J = 9.5$ Hz, 1H), 7.43 (s, 1H), 6.95 (dd, $J = 9.1, 2.1$ Hz, 1H), 6.71 (d, $J = 2.1$ Hz, 1H), 5.07 (s, 2H), 4.74 (s, 2H), 3.59 (q, $J = 6.9$ Hz, 4H), 1.64 (s, 6H), 1.18 (t, $J = 6.9$ Hz, 6H); ^{13}C NMR (100 MHz, DMSO- d_6): δ 179.8, 173.8, 158.6, 158.3, 154.7, 148.0, 147.2, 145.8, 140.9, 133.3, 125.4, 119.2, 113.4, 111.6, 109.2, 107.5, 96.2, 91.1, 70.6, 51.2, 49.9, 44.9, 24.7, 12.5. LC-HRMS (ESI): m/z calculated for $[M + H]^+$ 474.2023, found 474.2015.

2.2 Synthesis of I



A mixture of **1b** (380 mg, 1 mmol) and iodomethane (1.2 mL, 19.2 mmol) was stirred in acetone (6 mL) at 56°C for 11 h. Light yellow solid was produced and precipitated as reaction proceeded. After removal of the solvent, the crude product was washed with acetone for 5 times to afford the product as a light yellow solid **I** (470 mg, Yield: 90.2 %). m.p. $138.6 - 139.5^\circ\text{C}$; ^1H NMR (500 MHz, $\text{DMSO}-d_6$): δ 8.13 (dd, $J = 8.7, 2.1$ Hz, 1H), 8.06 (d, $J = 2.1$ Hz, 2H), 7.93 (d, $J = 8.9$ Hz, 2H), 7.84 (d, $J = 8.9$ Hz, 2H), 7.12 (d, $J = 8.7$ Hz, 1H), 6.90 (d, $J = 16.1$ Hz, 1H), 6.56 (d, $J = 16.1$ Hz, 1H), 3.45 – 3.89 (m, 4H), 3.60 (s, 9H), 1.46 (s, 3H), 1.15 (s, 3H); ^{13}C NMR (126 MHz, $\text{DMSO}-d_6$): δ 157.1, 146.5, 141.9, 140.4, 137.5, 130.1, 128.2, 127.6, 125.1, 120.7, 118.5, 111.9, 109.2, 63.3, 56.4, 48.9, 46.9, 30.7, 27.5, 20.1; LC-HRMS (ESI): m/z calculated for $[M + \text{H}]^+$ 394.2125, found 394.2125.

2.3 Synthesis of 3



A mixture of **1b** (400 mg, 1.05 mmol) and iodomethane (0.62 mL, 10 mmol) was stirred in dimethylformamide (2 mL) at 110°C for 36 h. Then the solvent was removed under reduced pressure and the crude mixture was precipitated as black solid. Purification of the crude mixture by chromatography (Petroleum ether / EtOAc = 6 / 1) afforded the product as a yellow solid **3** (20 mg, Yield: 5.4 %). m.p. $221.9 - 222.8^\circ\text{C}$; ^1H NMR (500 MHz, $\text{DMSO}-d_6$): δ 11.87 (s, 1H), 8.18 (dd, $J = 8.6, 2.1$ Hz, 1H), 8.10 (d, $J = 2.1$ Hz, 1H), 7.92 (d, $J = 8.9$ Hz, 2H), 6.93 (d, $J = 8.6$ Hz, 1H), 6.73 (d, $J = 8.9$ Hz, 2H), 6.18 (s, 1H), 3.07 (s, 6H), 1.51 (s, 6H); ^{13}C NMR (126 MHz, $\text{DMSO}-d_6$): δ 189.2, 170.6, 148.7, 142.7, 138.7, 129.7, 126.0, 118.6, 111.3, 109.0, 90.2, 46.9, 40.4, 28.0; LC-HRMS (ESI): m/z calculated for $[M + \text{H}]^+$ 352.1656, found 352.1659.

3. ^1H NMR spectra monitoring heating **1a-1f** in $\text{DMSO}-d_6$

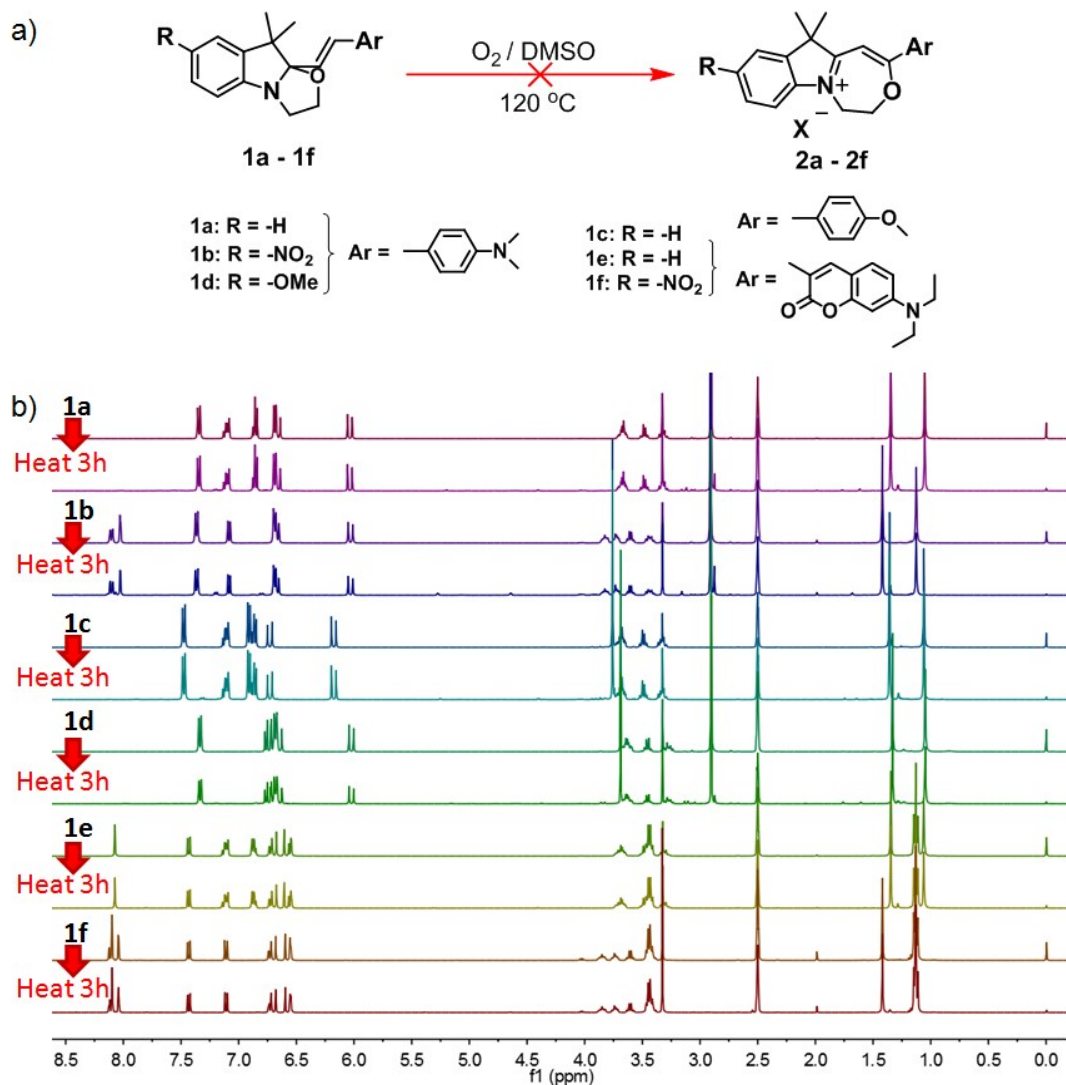


Figure S1. (a) Reaction of **1a-1f** in $\text{DMSO}-d_6$. (b) ^1H NMR spectra of **1a-1f** in $\text{DMSO}-d_6$ (5mg / 0.5 mL) before and after heating for 3 h at 120 °C.

4. Structural characterizations of intermediate product I of 1b reacting with CH₃I

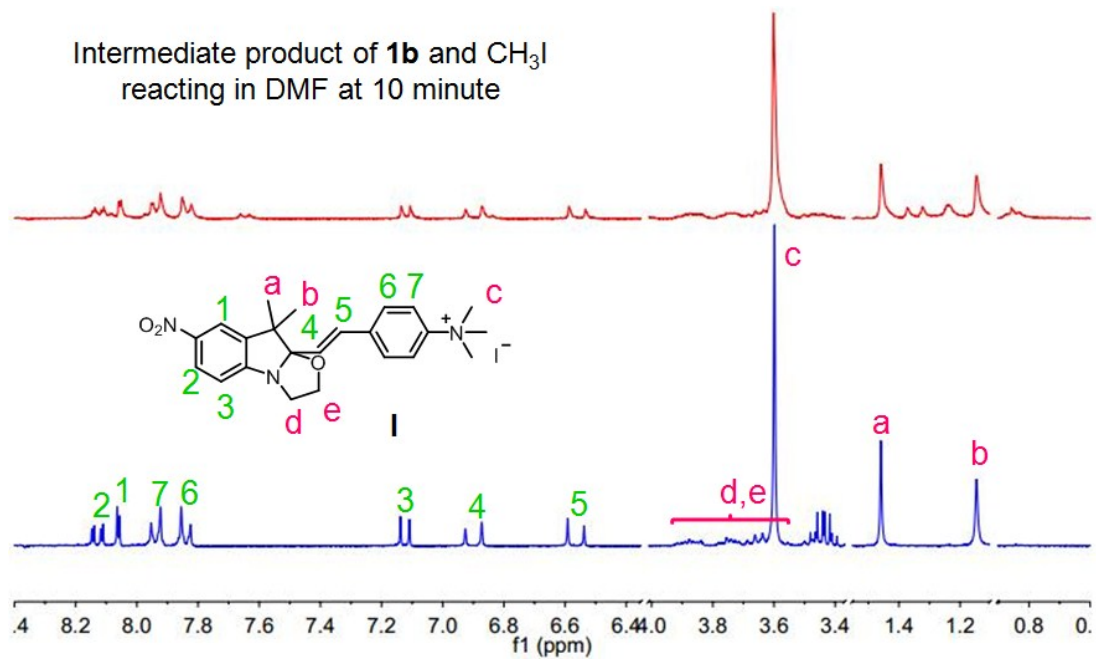


Figure S2. ¹H NMR spectra comparison between **I** (blue line) and intermediate products of **1b** and CH₃I reacting in DMF at 10 minutes (red line).

5. ^1H NMR spectra monitoring heating I in DMSO- d_6

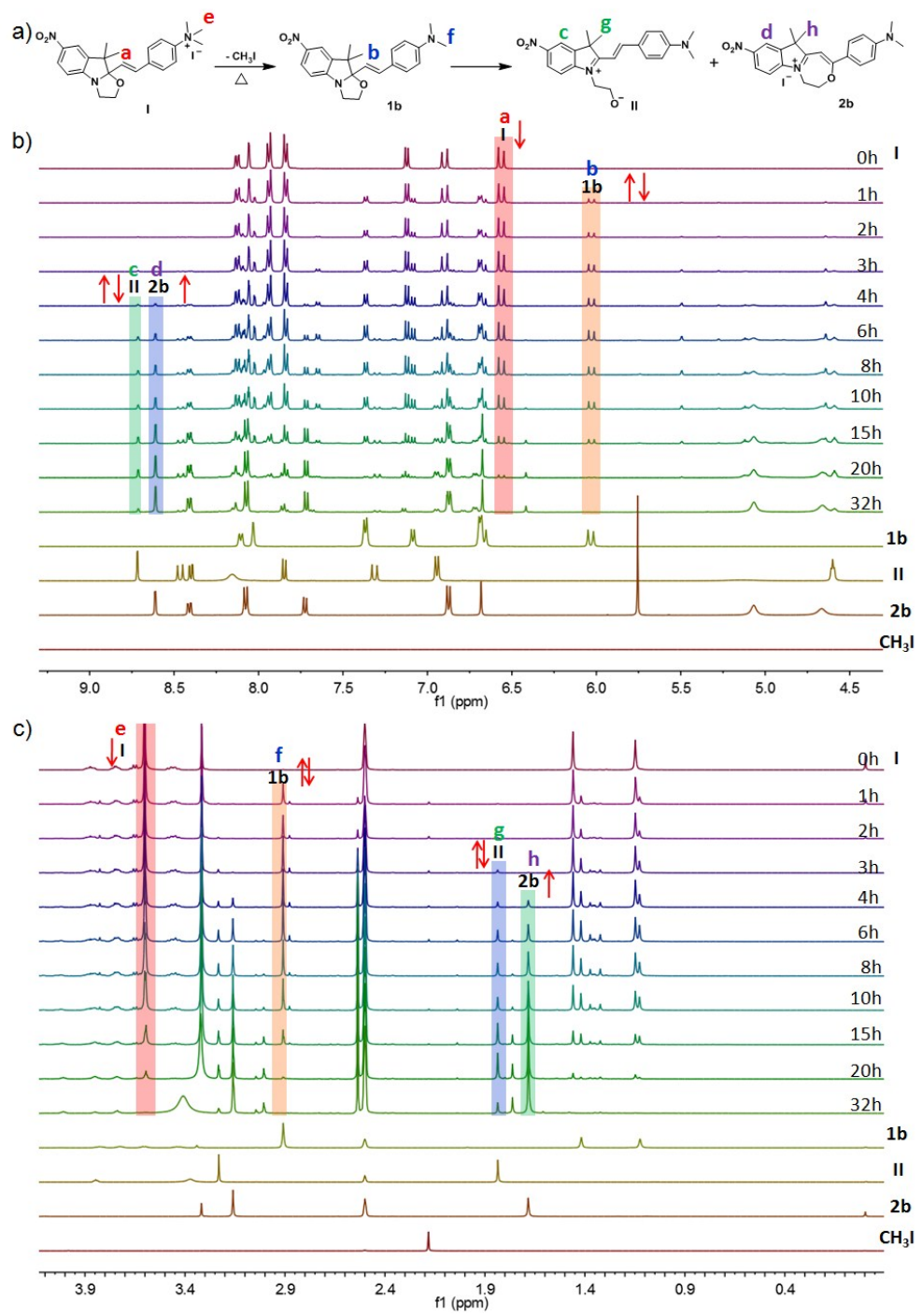


Figure S3. (a) Probable reaction process of **I** in DMSO- d_6 at 120 °C. (b) ^1H NMR spectra variation of **I** in DMSO- d_6 (5mg / 0.5 mL) in (b) low and (c) high magnetic fields at 120 °C with reaction time.

6. Photographs of heating CH₃I in DMSO

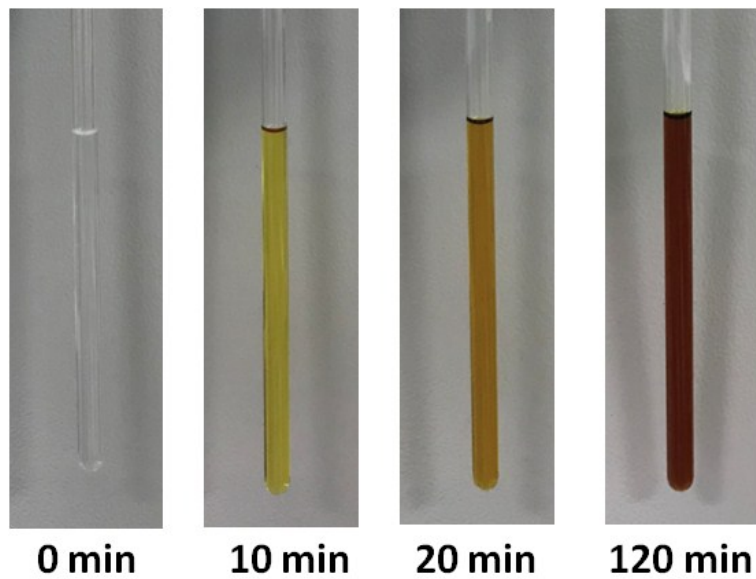


Figure S4. Photographs of CH₃I heated in DMSO over time in the dark at 120 °C.

The DMSO solution of CH₃I gradually changed from colorless to brown with heating time, which indicated the generation of I₂ from thermolysis of CH₃I.

7. HRMS and ^1H NMR spectra monitoring reaction of **1g** and CH_3I in DMF at 120°C

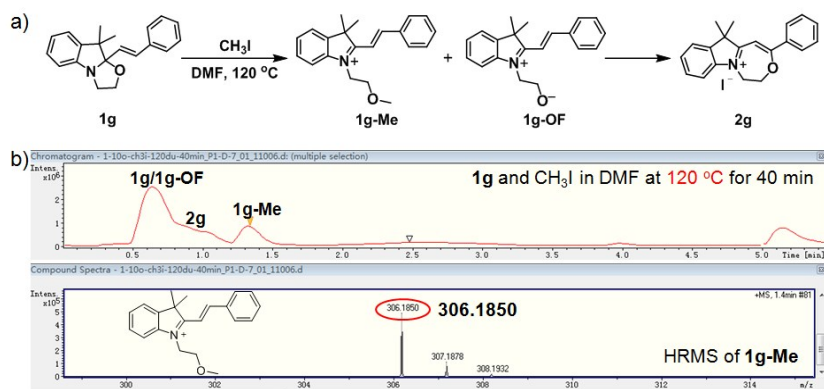


Figure S5. (a) Probable reaction process of **1g** and CH_3I in DMF at 120°C . (b) HRMS spectra of **1g** and CH_3I in DMF at 120°C for 40 min (above) and HRMS spectra of **1g-Me** (below).

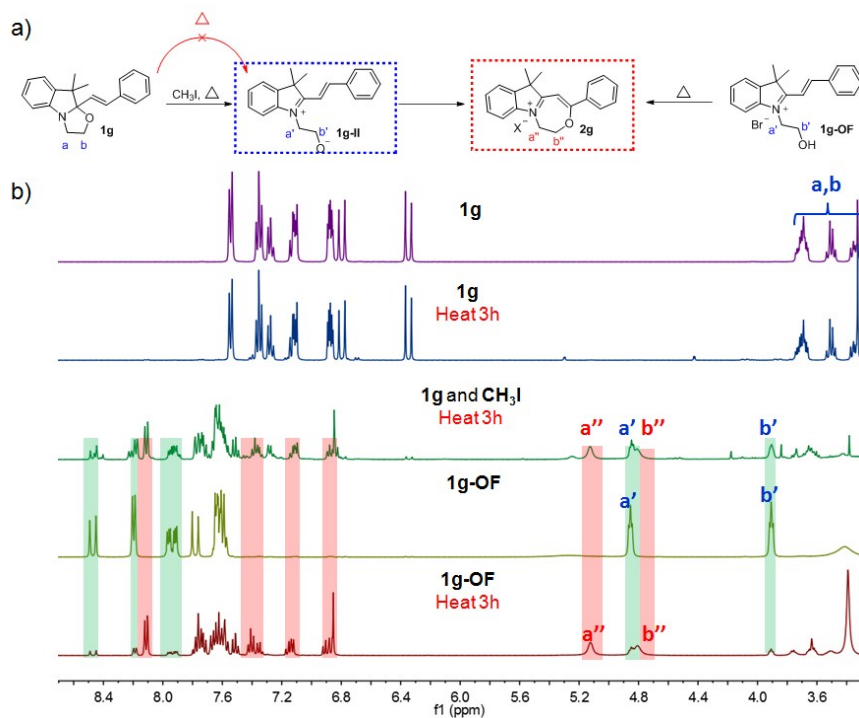


Figure S6. (a) Probable reaction process of **1g** and CH_3I in $\text{DMSO}-d_6$ at 120°C . (b) ^1H NMR spectra comparison of **1g** (purple), **1g** after heating 3 h (blue), **1g** and CH_3I after heating 3 h (green), **1g-OF** (yellow) and **1g-OF** after heating 3 h (dark red) (5 mg / 0.5 mL in $\text{DMSO}-d_6$).

8. ^1H NMR spectra monitoring heating **1b**-OF in $\text{DMSO}-d_6$

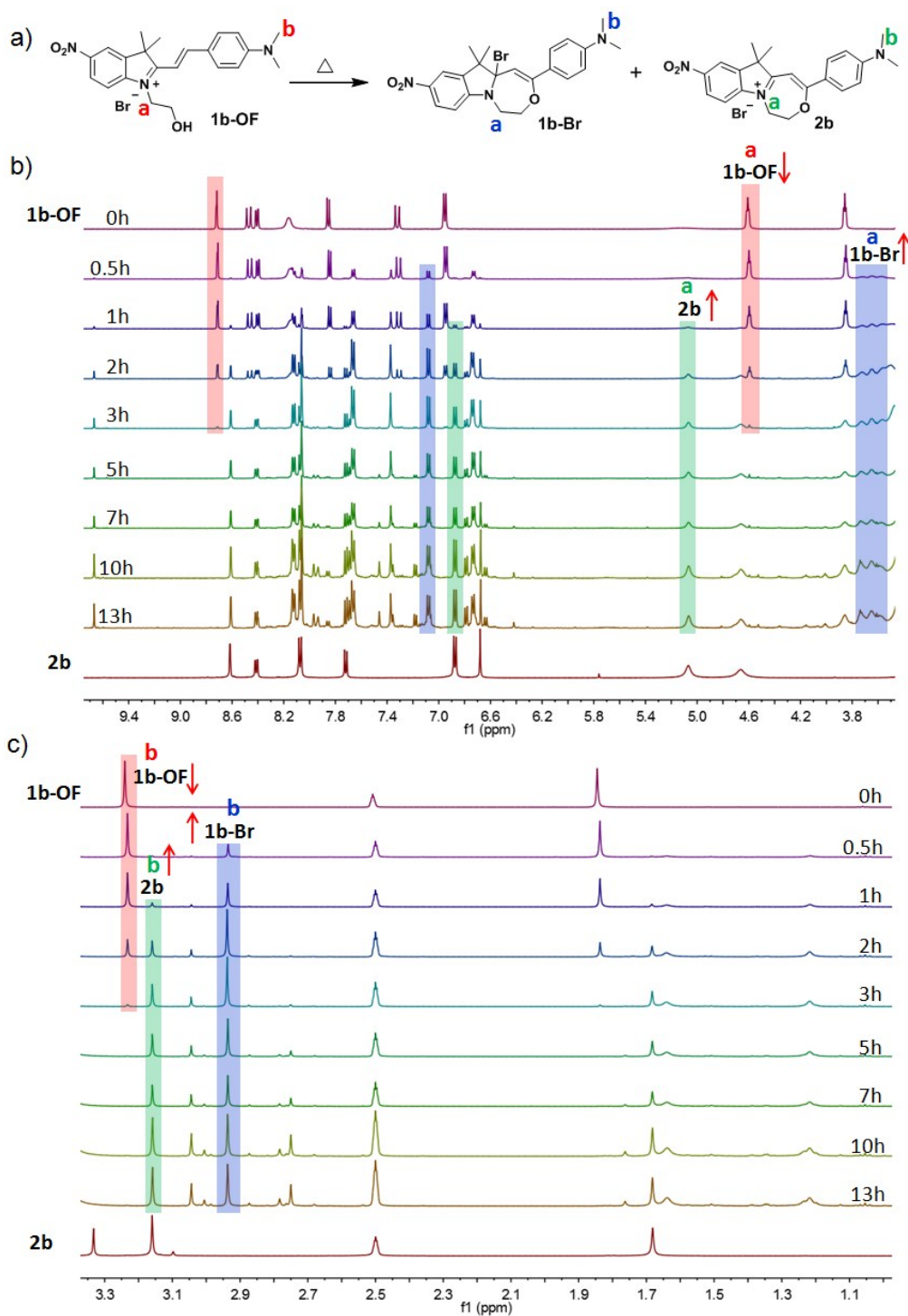


Figure S7. (a) Probable reaction process of **1b**-OF in $\text{DMSO}-d_6$ at $120\text{ }^\circ\text{C}$. (b) ^1H NMR spectra variation of **1b**-OF in $\text{DMSO}-d_6$ (5 mg / 0.5 mL) in (b) low and (c) high magnetic fields at $120\text{ }^\circ\text{C}$ with reaction time.

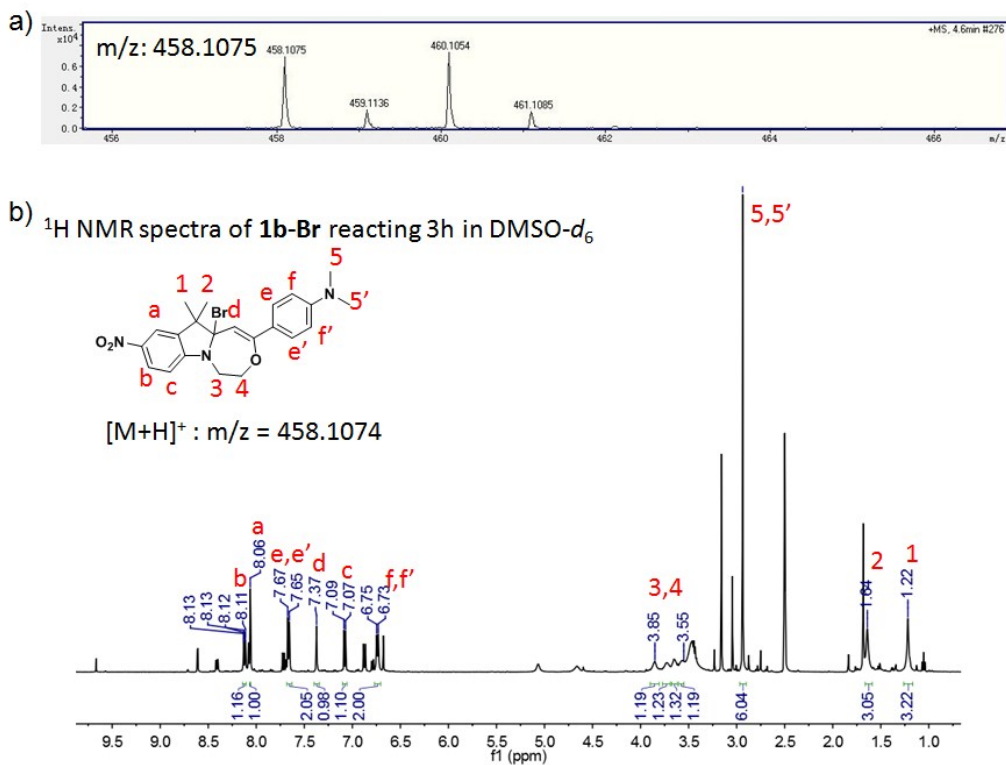


Figure S8. (a) HRMS spectrum of **1b-Br** and (b) ^1H NMR spectrum of **1b-OF** in $\text{DMSO}-d_6$ (5 mg / 0.5 mL) after reacting 3h at 120 °C and the speculated structure of **1b-Br**.

9. Comparison of **1b**-OF reaction in DMSO under aerobic and anaerobic conditions

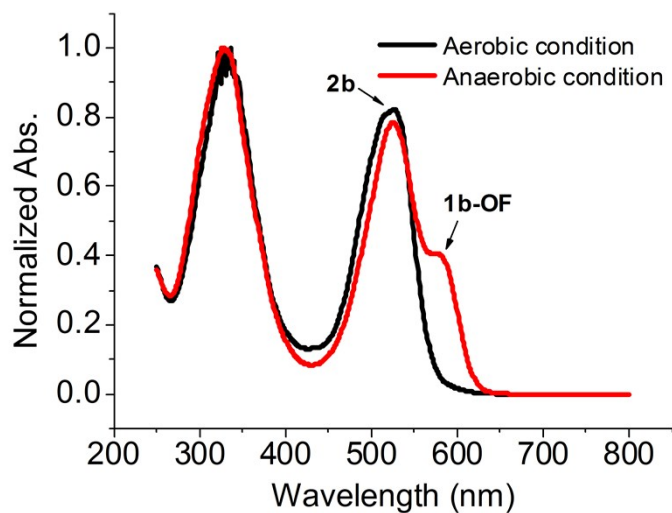


Figure S9. The UV-Vis spectra of the diluted reaction solution of **1b**-OF after heating for 4 hours in DMSO under aerobic (black line) and anaerobic (red line) conditions.

1b-OF could be oxidized to **2b** both under aerobic and anaerobic condition, but it exhibits a slower reaction rate under anaerobic condition within the same reaction time of 4 h. It proved that except O₂, DMSO also works as oxidant in this reaction.

10. Reaction of **1a**-OF with H₂O₂ in DMF

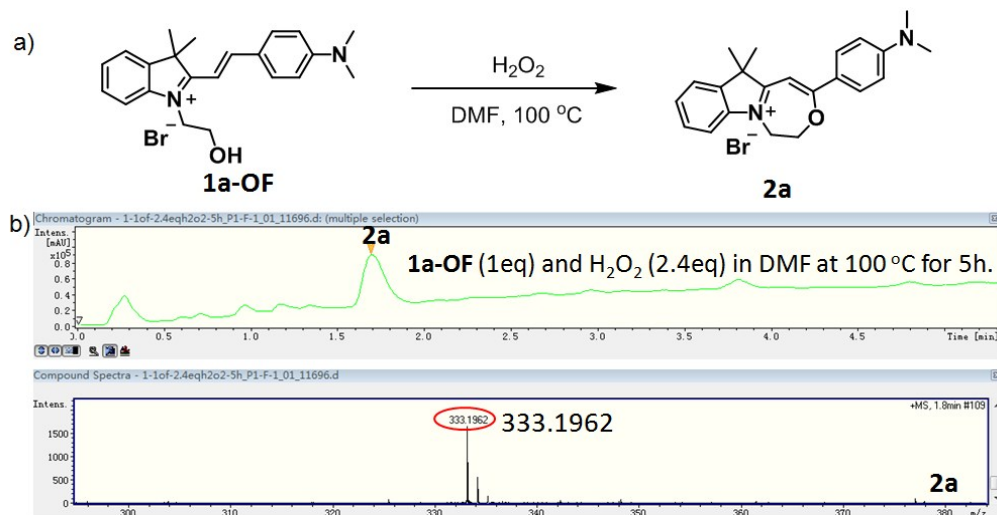


Figure S10. (a) Reaction process of **1a**-OF and H₂O₂ in DMF solution at 100 °C. (b) HRMS spectra for reaction solutions of **1a**-OF (1.0 eq) and H₂O₂ (2.4 eq) in DMF solution at 100 °C for 5 h.

11. Reaction of **1b**-OF in DMSO/DMF solutions with addition of radical inhibitor BHT

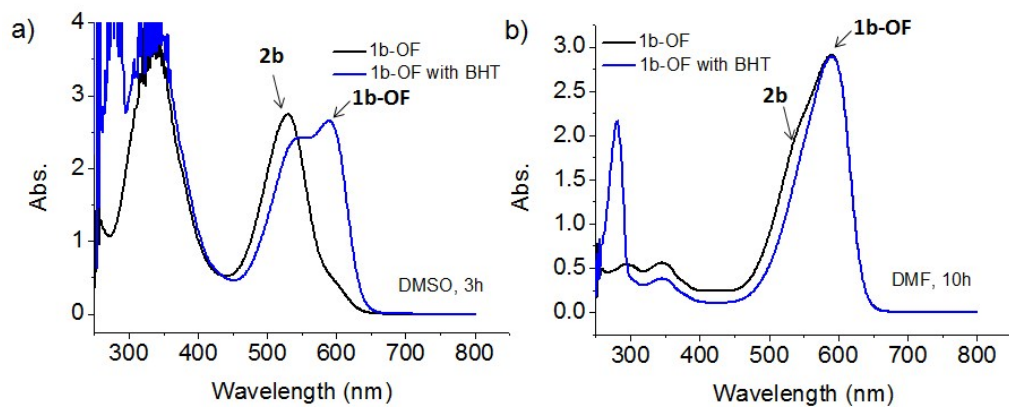


Figure S11. UV-Vis spectra for the diluted reaction solutions of **1b**-OF with (blue line) and without (black line) addition of butylated hydroxytoluene (BHT) in (a) DMSO and (b) DMF solutions, respectively.

12. HRMS spectra for reaction solutions of **1b** with NIS, NBS and NCS

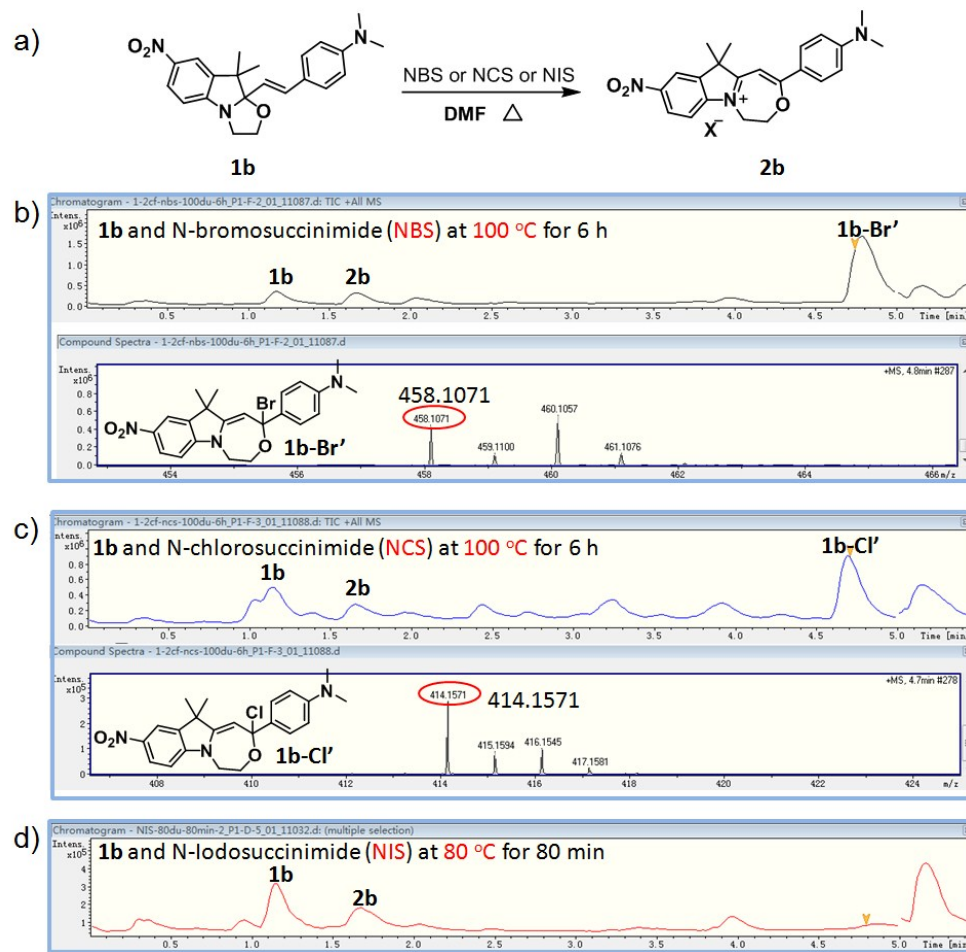


Figure S12. (a) Reaction process of **1b** (1.0 eq) with N-iodosuccinimide (NIS), N-bromosuccinimide (NBS), and N-chlorosuccinimide (NCS) (1.2 eq) in DMF solution. (b) – (d) HRMS spectra for reaction solutions of **1b** with NBS at 100 °C for 6 h, NCS at 100 °C for 6 h and NIS at 80 °C for 80 min, respectively.

13. Crystal data and structure refinement for **2a**, **2b**, **2c** and **3**

Single crystals of **2a**, **2b**, **2c** and **3** were all obtained by vapor diffusion of n-hexane into their acetonitrile solutions of **2a**, **2b** and **2c**. Single crystal of **3** was obtained by slow evaporation in mixed solution of n-hexane and EtOAc.

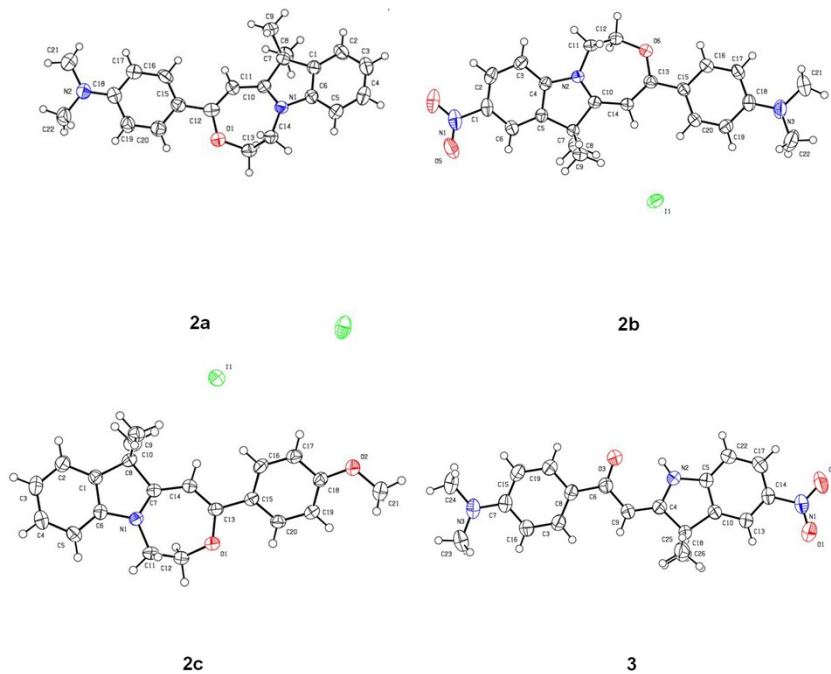


Figure S13. Single-crystal X-ray structures of **2a**, **2b**, **2c** and **3** (50 % probability ellipsoids). The anion in **2a**, **2b** and **2c** is I^- .

Table S1. Summary of crystal data and intensity collection parameters for **2a**, **2b**, **2c** and **3**.

Compound	2b	2a	2c	3
Formula	C ₂₂ H ₂₄ IN ₃ O ₃	C ₂₂ H ₂₅ IN ₂ O	C ₂₁ H ₂₂ INO ₂	C ₂₀ H ₂₁ N ₃ O ₃
Formula mass	505.34	460.34	447.29	351.40
Space group	monoclinic P 21/n	monoclinic P 21/c	triclinic P-1	monoclinic P 21/c
<i>a</i> / Å	6.4834 (13)	20.1317(10)	9.4276(5)	10.118(2)
<i>b</i> / Å	23.560 (5)	7.4780(4)	10.1879(5)	9.1993(18)
<i>c</i> / Å	14.458(3)	13.4306(6)	11.1539(6)	20.098(4)
<i>α</i> / °	90	90	111.6410(10)	90
<i>β</i> / °	100.21(3)	94.394(2)	97.790(2)	100.49(3)
<i>γ</i> / °	90	90	99.874(2)	90
V / Å ³	2173.4(8)	2015.96(17)	957.65(9)	1839.4(7)
Z	4	4	2	4
ρ/ g.cm ⁻³	1.544	1.517	1.551	1.269
μ/ mm ⁻¹	1.501	1.601	1.685	0.087
F000	1016	928	448	744.0
Temp, (K)	293(2) K	273(2) K	273(2) K	293 K
No. of reflns. collected	19917	12417	6501	17394
No. of unique reflns.	4975	3542	3553	4194
R _{int}	0.0276	0.0437	0.0215	0.0325
Final <i>R</i> 1 values (<i>I</i> > 2σ(<i>I</i>))	0.0320	0.0378	0.0318	0.0466
Final <i>wR</i> (<i>F</i> ²) values (<i>I</i> > 2σ(<i>I</i>))	0.0724	0.0777	0.0732	0.1199
Final <i>R</i> 1 values (all data)	0.0405	0.0576	0.0398	0.0690
Final <i>wR</i> (<i>F</i> ²) values (all data)	0.0774	0.0869	0.0789	0.1289
Goodness of fit on <i>F</i> ²	1.124	1.023	1.015	1.057
CCDC numbers	1562292	1562290	1562291	1571735

14. Spectral data of 1a-OF-1f-OF and 2a-2f in DCM solutions and PMMA films

14.1 Maximum absorption wavelength, maximum emission wavelength and molar absorption coefficient of 1a-OF-1f-OF and 2a-2f.

Table S2. Spectral data including maximum absorption wavelength, maximum emission wavelength and molar absorption coefficient of **1a-OF** to **1f-OF** and **2a** to **2f** (a) in DCM solutions (3.0×10^{-5} M) and (b) in PMMA films (**2e** is 0.6% and others are 1.0 % weight percent).

a)	Solution (in DCM)	$\lambda_{1,\text{abs}}$ (nm)	$\lambda_{1,\text{em}}$ (nm)	ϵ_1 (L/mol·cm)	Solution (in DCM)	$\lambda_{2,\text{abs}}$ (nm)	$\lambda_{2,\text{em}}$ (nm)	ϵ_2 (L/mol·cm)	$\Delta\lambda_{\text{abs}} =$ $\lambda_{2,\text{abs}} - \lambda_{1,\text{abs}}$	$\Delta\lambda_{\text{em}} =$ $\lambda_{2,\text{em}} - \lambda_{1,\text{em}}$	$\Delta\epsilon = \epsilon_2 - \epsilon_1$ (L/mol·cm)
	1a-OF	559	592	86530	2a	517	557	84190	-42	-35	-2340
	1b-OF	593	624	137380	2b	535	578	90450	-58	-47	-46930
	1c-OF	445	482	36760	2c	427	480	42420	-18	-2	5660
	1d-OF	561	603	73550	2d	522	565	66130	-39	-38	-7420
	1e-OF	622	666	87100	2e	572	609	105710	-50	-57	18610
	1f-OF	666	701	104680	2f	598	642	82670	-68	-59	-22010

b)	Film (in PMMA)	$\lambda_{1,\text{abs}}$ (nm)	$\lambda_{1,\text{em}}$ (nm)	Film (in PMMA)	$\lambda_{2,\text{abs}}$ (nm)	$\lambda_{2,\text{em}}$ (nm)	$\Delta\lambda_{\text{abs}} =$ $\lambda_{2,\text{abs}} - \lambda_{1,\text{abs}}$	$\Delta\lambda_{\text{em}} =$ $\lambda_{2,\text{em}} - \lambda_{1,\text{em}}$
	1a-OF	547	601	2a	495	563	-52	-38
	1b-OF	586	631	2b	517	589	-69	-42
	1c-OF	433	-	2c	415	503	-18	-
	1d-OF	539	609	2d	493	573	-46	-36
	1e-OF	603	677	2e	549	614	-54	-63
	1f-OF	655	700	2f	568	640	-87	-60

14.2 Measurement of molar absorption coefficient of 1a-OF-1f-OF and 2a-2f.

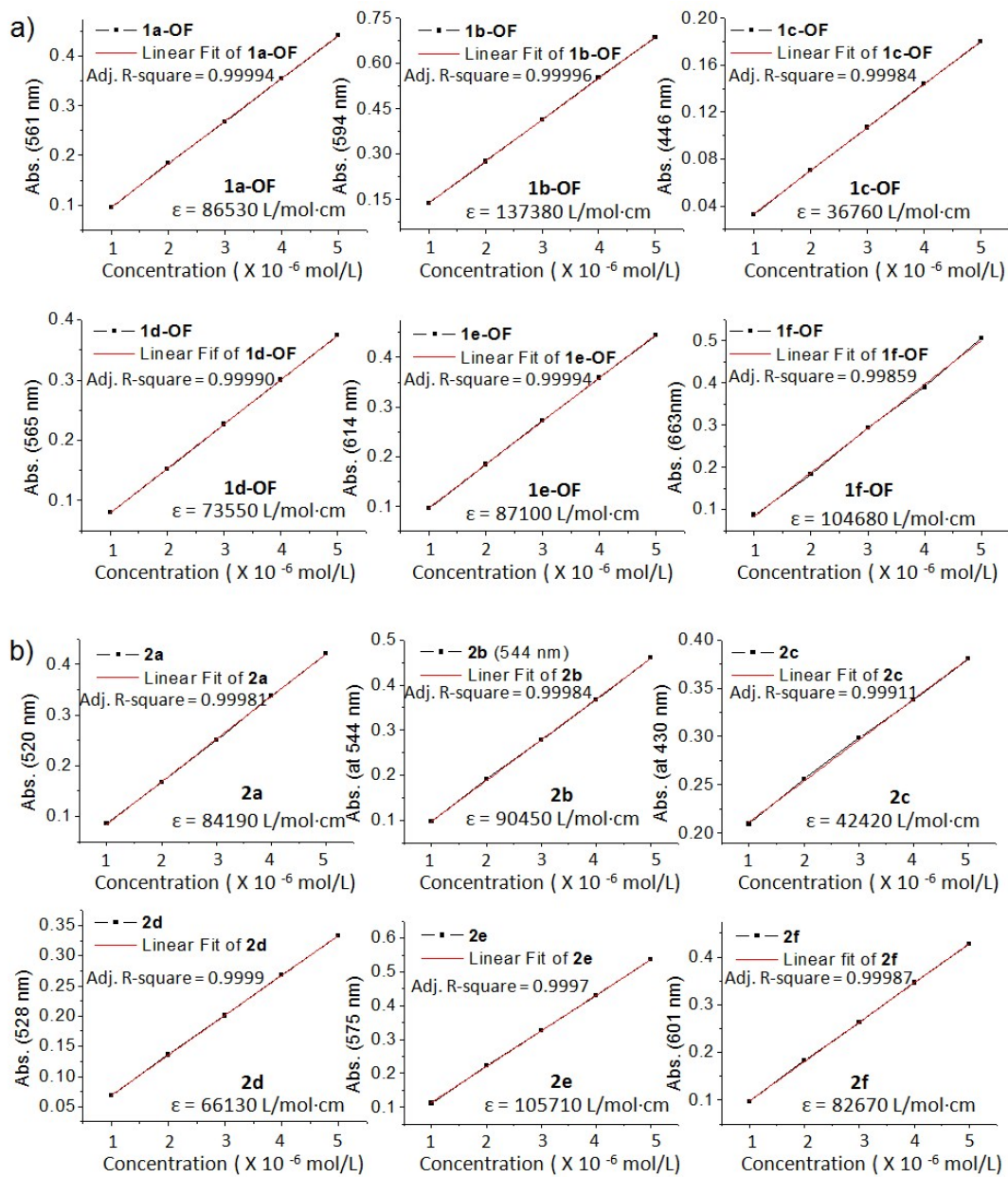


Figure S14. Plots of molar absorption coefficient for (a) 1a-OF-1f-OF and (b) 2a-2f in DCM.

14.3 Fluorescent lifetime measurements of **1a**-OF-**1f**-OF and **2a**-**2f**.

Table S3. Fluorescence lifetime of **1a**-OF to **1f**-OF in DCM solutions (5.0×10^{-5} M) and PMMA films (1.0 % weight percent). ^{a)} $\lambda_{\text{ex}} = 400$ nm. ^{b)} $\lambda_{\text{ex}} = 375$ nm.

		$\tau_1(\text{ns})$	$\tau_2(\text{ns})$	$\tau_{\text{avg}}(\text{ns})$	χ^2
1a -OF	solution ^{a)}	0.34	2.54	0.58	1.363
	film ^{a)}	0.94	2.17	1.38	1.119
1b -OF	solution ^{a)}	0.61	3.25	1.36	1.653
	film ^{a)}	0.72	2.59	1.03	1.402
1c -OF	solution ^{a)}	0.26	2.59	0.49	1.309
	film ^{a)}	0.71	2.25	1.60	1.253
1d -OF	solution ^{a)}	0.30	2.73	0.56	1.381
	film ^{a)}	0.70	1.84	1.10	1.253
1e -OF	solution ^{b)}	1.84	-	1.84	1.643
	film ^{a)}	2.08	14.1	2.27	1.395
1f -OF	solution ^{b)}	3.67	-	3.67	1.419
	film ^{a)}	2.29	15.73	2.56	1.182

Table S4. Fluorescence lifetime of **2a** to **2f** in DCM solutions (5.0×10^{-5} M) and PMMA films (1.0 % weight percent). ^{a)} $\lambda_{\text{ex}} = 400$ nm. ^{b)} $\lambda_{\text{ex}} = 375$ nm.

		$\tau_1(\text{ns})$	$\tau_2(\text{ns})$	$\tau_{\text{avg}}(\text{ns})$	χ^2
2a	solution ^{b)}	1.70	-	1.70	1.991
	film ^{a)}	1.99	4.23	2.71	1.378
2b	solution ^{b)}	1.53	-	1.53	1.577
	film ^{a)}	1.14	2.53	1.74	1.360
2c	solution ^{b)}	1.53	-	1.53	1.790
	film ^{a)}	0.97	2.22	1.62	1.147
2d	solution ^{b)}	1.38	-	1.38	2.381
	film ^{a)}	1.82	3.59	2.31	1.108
2e	solution ^{b)}	3.27	-	3.27	1.722
	film ^{a)}	1.93	4.06	2.29	1.234
2f	solution ^{b)}	2.56	-	2.56	1.445
	film ^{a)}	1.08	2.22	1.81	1.704

15. Fluorescent photographs of solid powders of **1a-OF-**1f**-OF and **2a**-**2f****

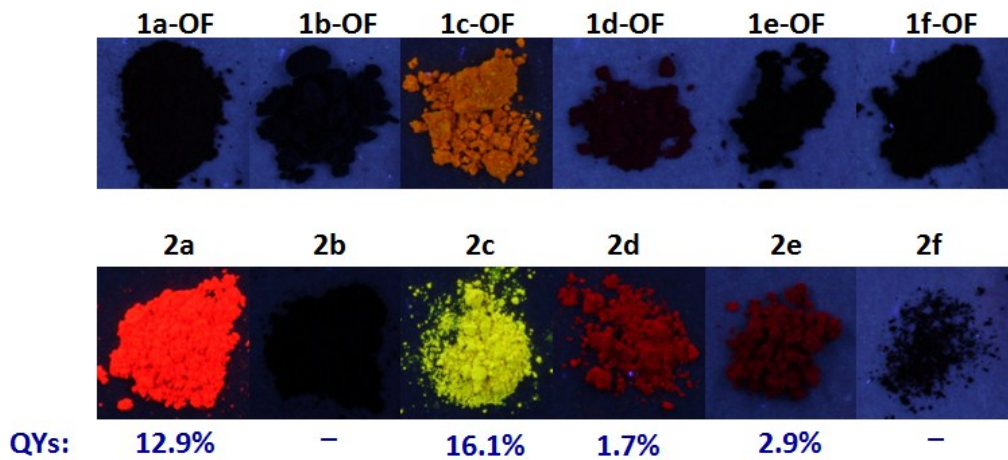


Figure S15. Fluorescent photographs of solid powder of **1a**-OF-**1f**-OF (above) and **2a**-**2f** (below) under 365 nm handheld UV lamp, and the absolute fluorescence quantum yields of **2a**, **2c**, **2d** and **2e**.

16. Solvent polarity effects on optical properties of 2a-2f

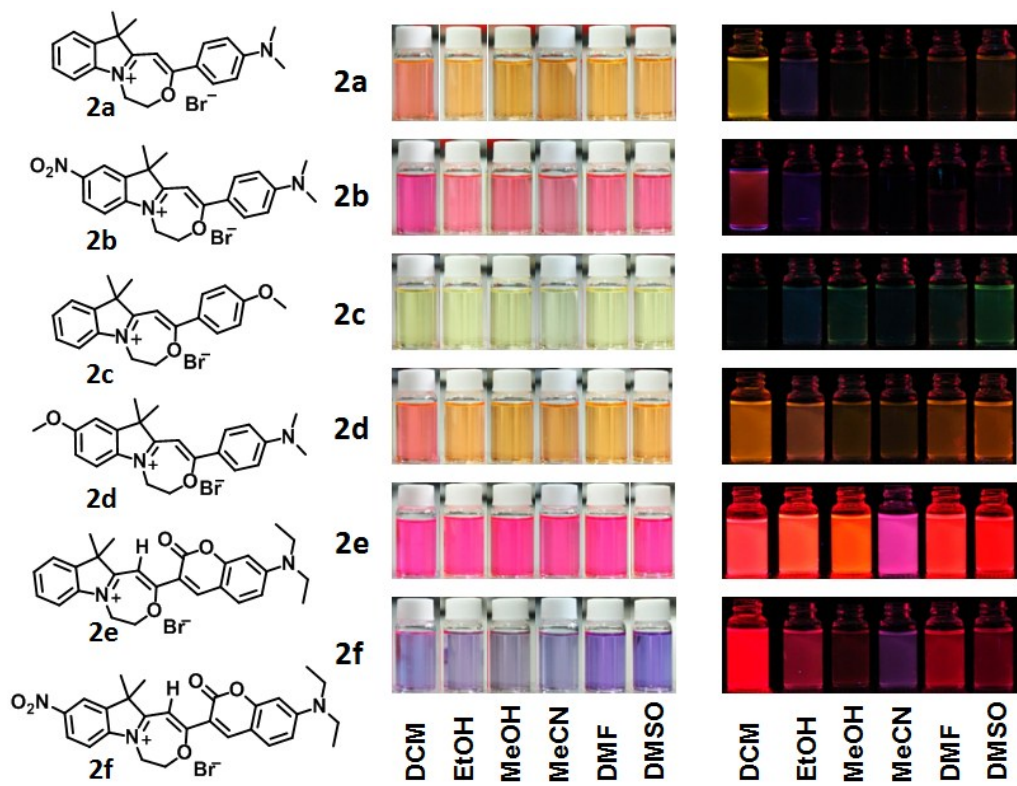


Figure S16. Structures and photographs of **2a-2f** in different solvents (1.0×10^{-5} M) under visible and UV light by 365 nm handheld UV lamp.

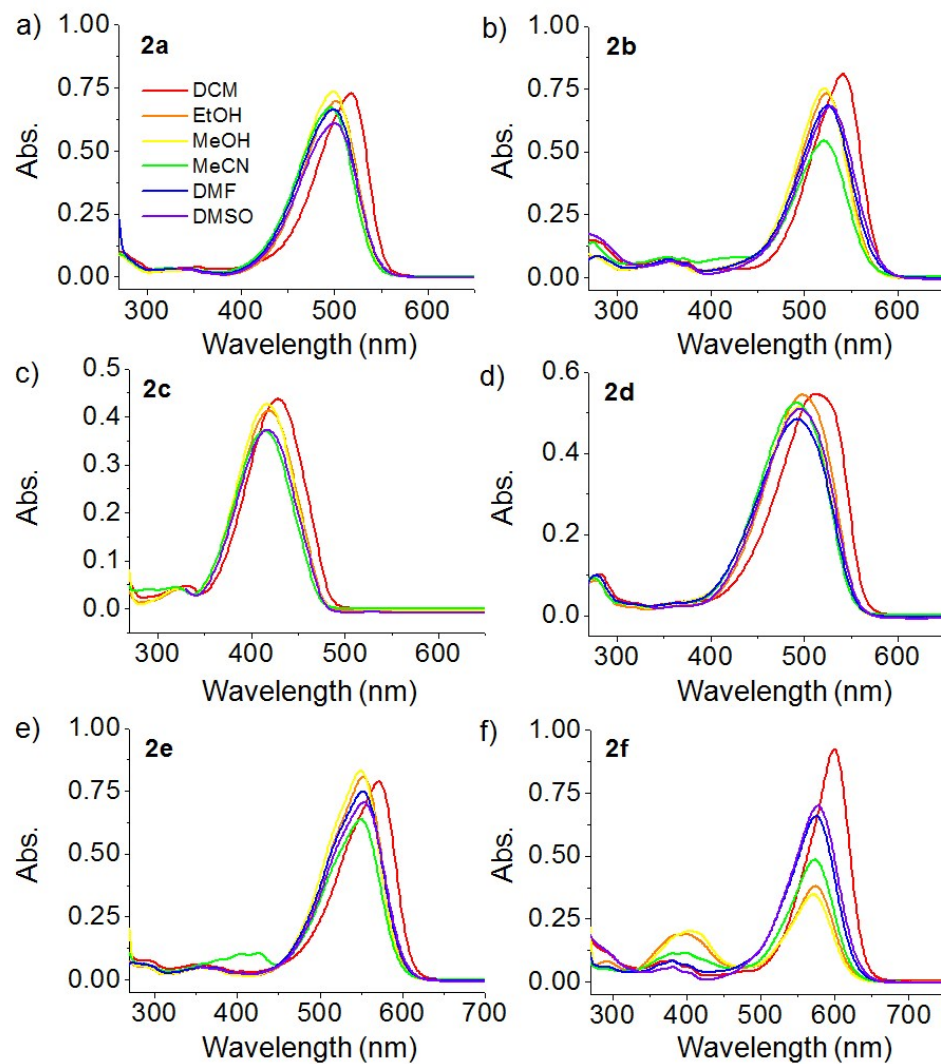


Figure S17. UV-Vis spectra of **2a-2f** in different solvents (1.0×10^{-5} M).

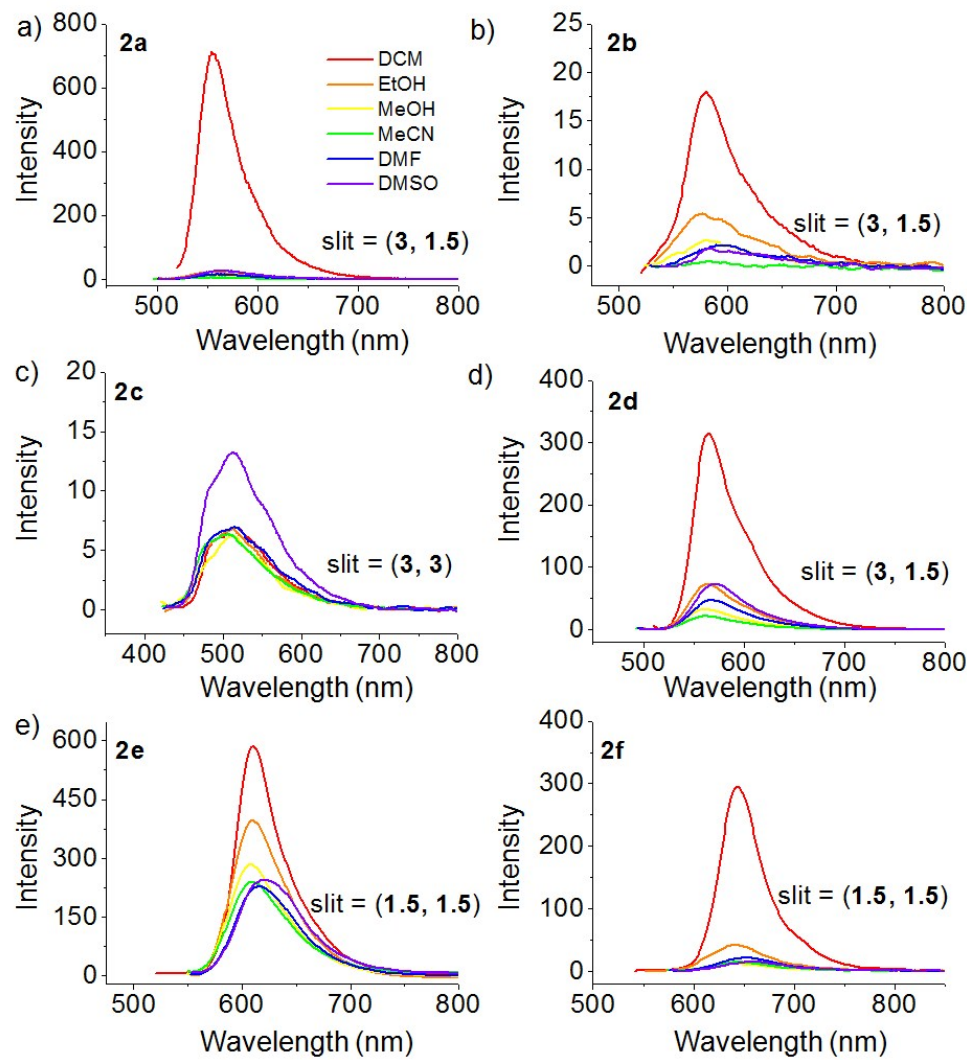


Figure S18. Fluorescence emission spectra of **2a-2f** in different solvents (1.0×10^{-5} M).

17. Photographs, UV-Vis spectra and fluorescent spectra of 2a-2f in PMMA with different weight percent

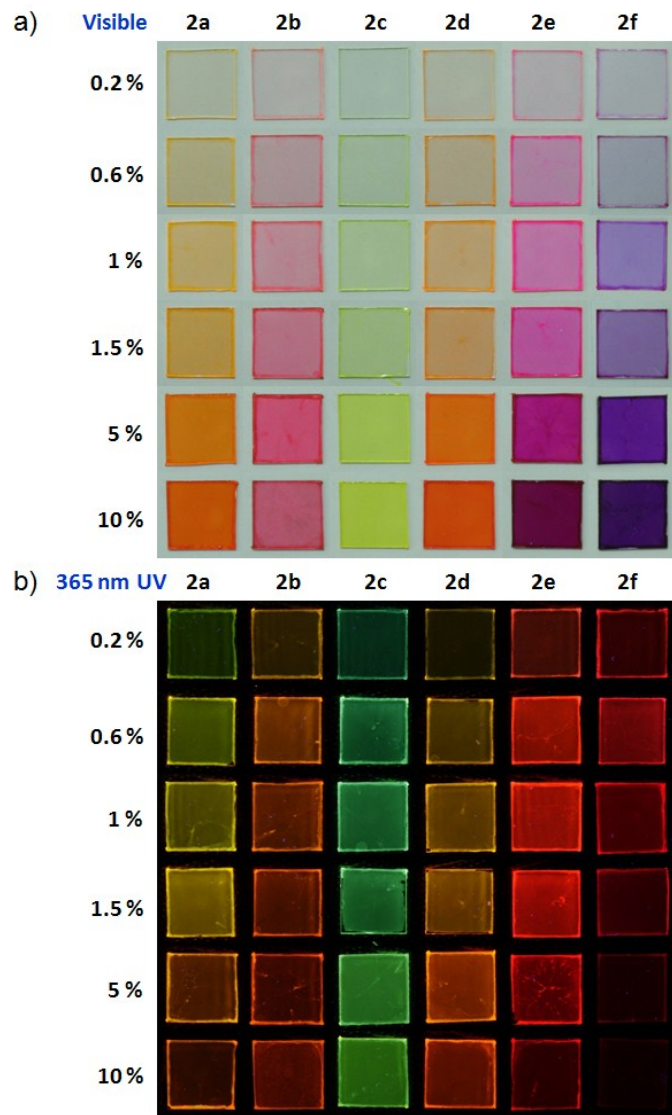


Figure S19. Photographs of spin-coated **2a-2f** PMMA films with weight percent of 0.2%, 0.6%, 1%, 1.5%, 5% and 10% respectively (a) under visible light and (b) 365 nm handheld UV lamp.

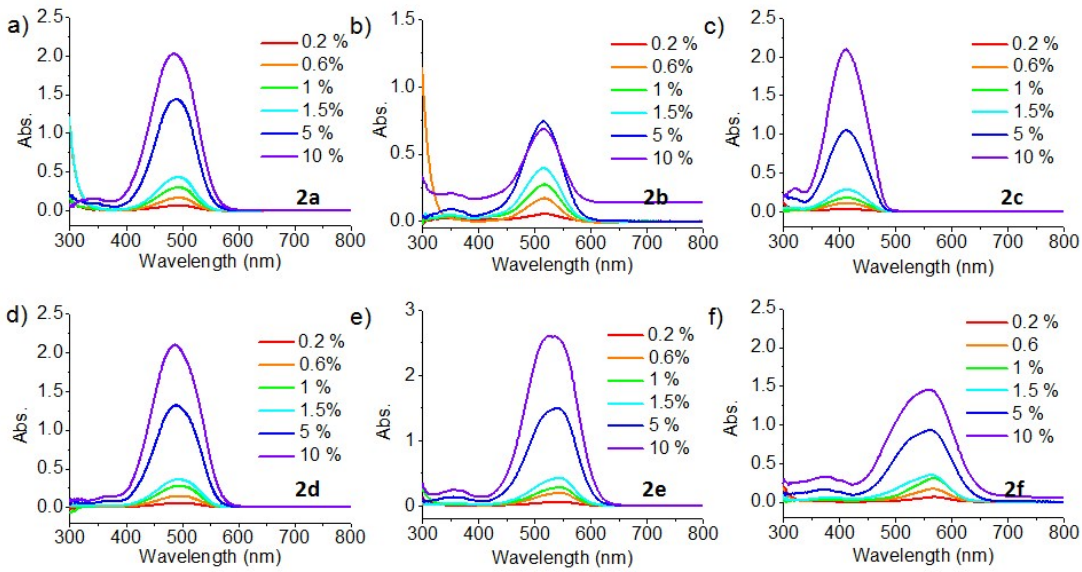


Figure S20. (a) - (f) UV-Vis spectra of spin-coated **2a-2f** PMMA films with weight percent of 0.2%, 0.6%, 1%, 1.5%, 5% and 10% respectively.

2b is not fully soluble when the weight percent reaches 10%, so the baseline increased.

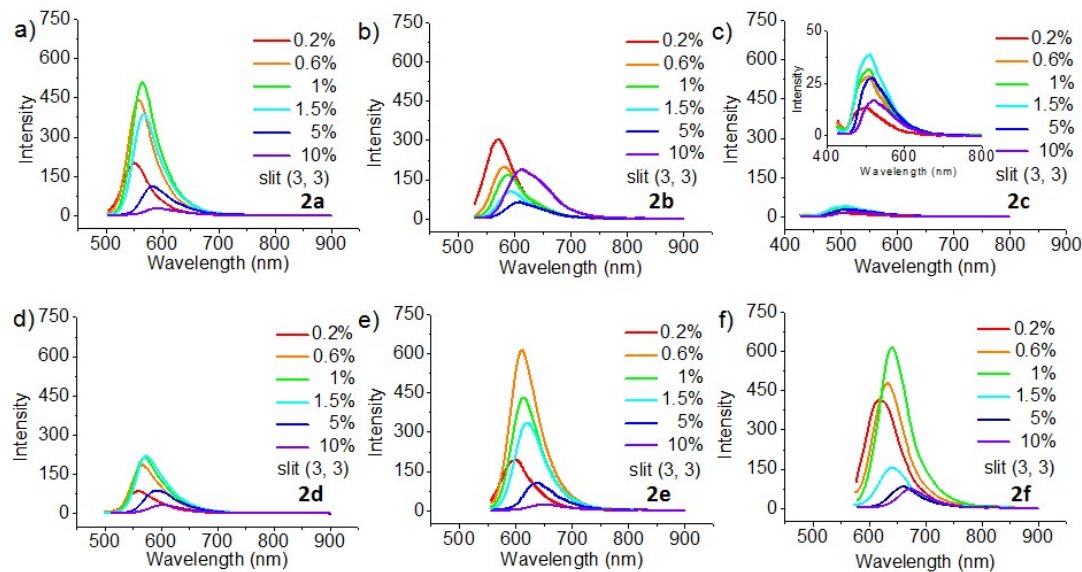


Figure S21. (a) - (f) Fluorescence spectra of **2a-2f** in PMMA films by spinning coating of different weight percent (0.2%, 0.6%, 1%, 1.5%, 5% and 10%).

18. Comparison of fluorescence quantum efficiency of 2a and 2c with I⁻, Br⁻ and PF₆⁻

Synthesis of 2a and 2c with different anions (I⁻ or PF₆⁻): **2a** (I⁻)/**2c** (I⁻) were obtained by the reaction of **1a**/**1c** with CH₃I in DMSO at 120 °C. **2a** (PF₆⁻)/**2c** (PF₆⁻) were obtained by counterion exchange with the bromide anions. The synthetic method is that we synthesized the crude product **2a** (Br⁻) and **2c** (Br⁻) in DMSO, respectively and added 15 equivalents of ammonium hexafluorophosphate into the DMSO solution. After stirring 20 minutes and adding saturated saline, the crude product **2a** and **2c** with hexafluorophosphate anion precipitated out. The product were purified by chromatography (dichloromethane / methanol = 60 / 1).

Structures confirmation of **2a (PF_6^-) and **2c** (PF_6^-)**: The ^1H NMR spectra in Fig. S19 indicated that **2a** (PF_6^-) and **2c** (PF_6^-) may be obtained, but the anions can't be determined. Moreover, compared to **2a** (Br^-) and **2c** (Br^-), the significantly reduced mobile phase polarity when doing chromatography, as well as 1~4 nm red shift of absorption spectra confirmed that we indeed obtained product **2a** and **2c** with PF_6^- and I^- (Fig. S20).

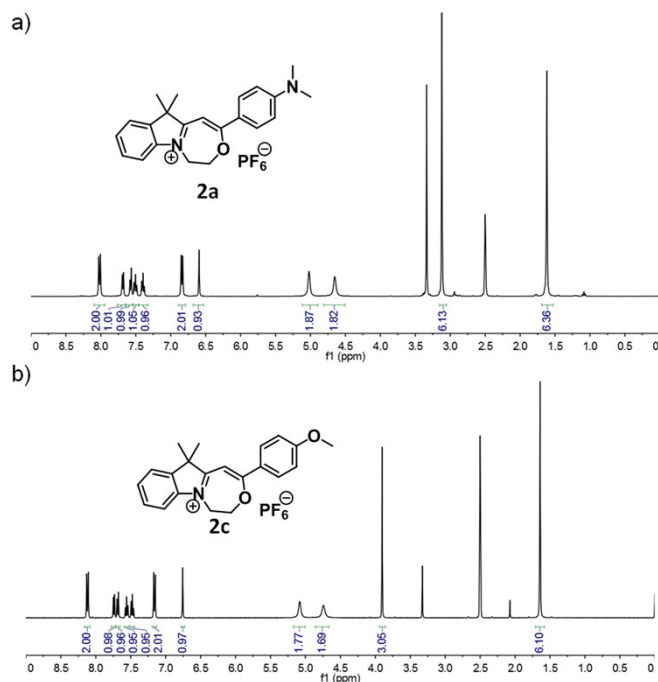


Figure S22. ^1H NMR spectra of **2a** and **2c** with hexafluorophosphate anion.

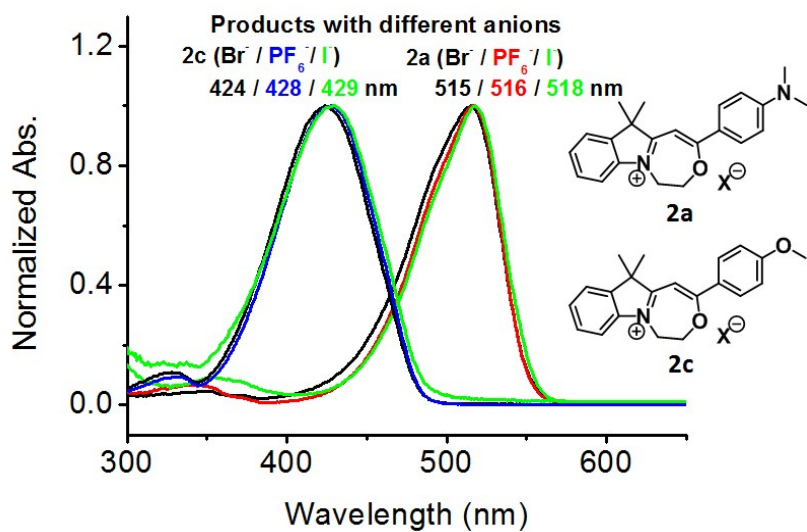


Figure S23. Normalized UV-Vis spectra of **2a** and **2c** with I⁻, Br⁻ and PF₆⁻ in dichloromethane, respectively.

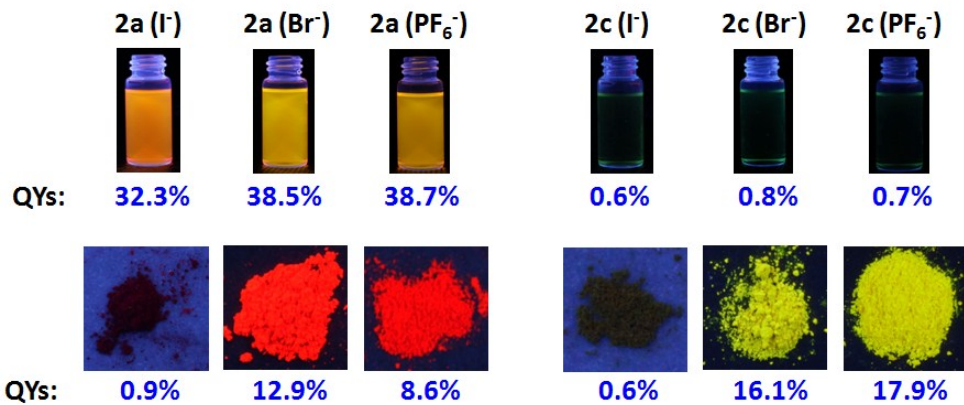


Figure S24. Comparison of photos and absolute fluorescence quantum yields of **2a** and **2c** with I⁻, Br⁻ and PF₆⁻ in dichloromethane and in solid states, respectively.

19. Theoretical calculations of energy levels of frontier molecular orbitals for ground states of **2a-2f**

All the Density functional theory (DFT) calculations were carried out using the GAUSSIAN 09 series of programs.^{S2} DFT and B3LYP with a standard 6-31g (d) basis set were used for geometry optimizations of ground states of **2a-2f**. And the vibrational spectrum of each molecule was calculated at the same level of theory to ensure that all of the structures correspond to the true minima of the potential energy surface.

	2a	2b	2c	2d	2e	2f
LUMO (eV)	-5.30	-5.68	-5.62	-5.16	-5.42	-5.74
HOMO (eV)	-8.17	-8.48	-8.83	-7.95	-8.03	-8.29
Band gap (eV)	2.87	2.80	3.21	2.79	2.61	2.55

Table S5. Calculated energy levels of frontier molecular orbitals for ground states of **2a-2f**.

20. Photostability and thermal stability of **2a-2f**

20.1 Measuring the photostability of **2a-2f** in dichloromethane.

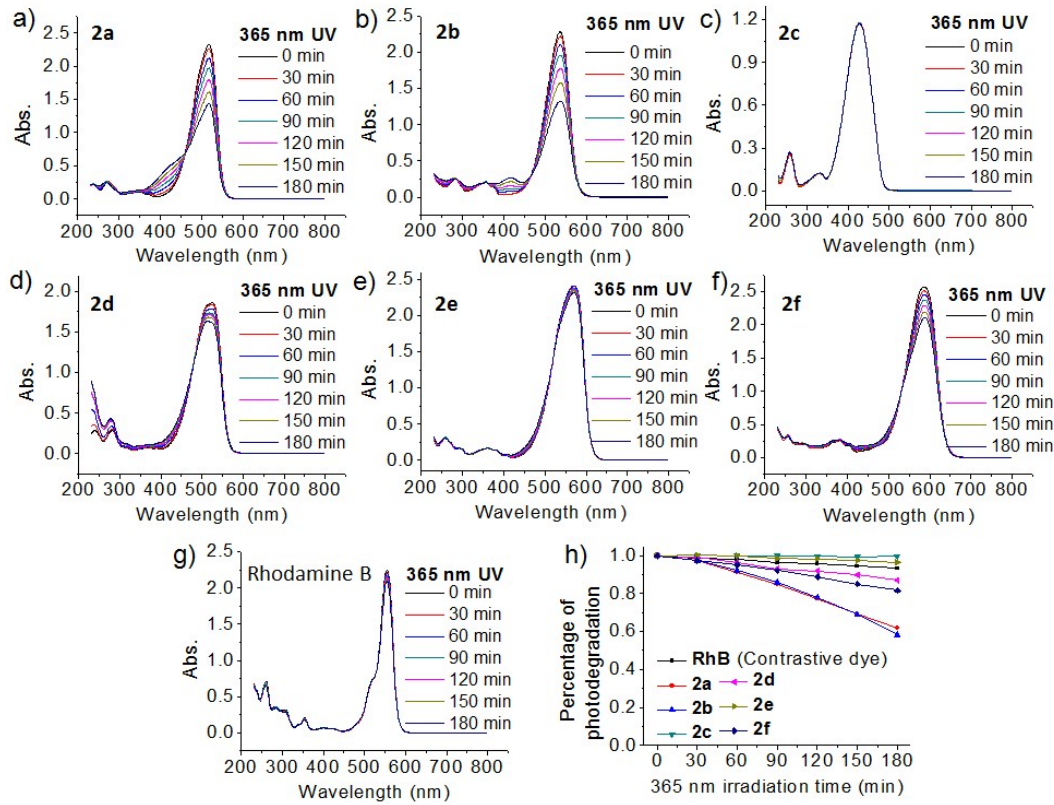


Figure S25. Measuring the photostability of **2a-2f**. (a) ~ (g) UV-Vis absorption spectra of **2a-2f** and the Rhodamine B (a commercial dye) in dichloromethane (2.0×10^{-5} M) with different UV irradiation time by 365 nm hand hold UV lamp (power: 12 W, distance: 5 cm). (h) Remaining percentage of the dyes **2a-2f** and Rhodamine B after photodegradation.

20.2 Measuring the thermal stability for solids of 2a-2f.

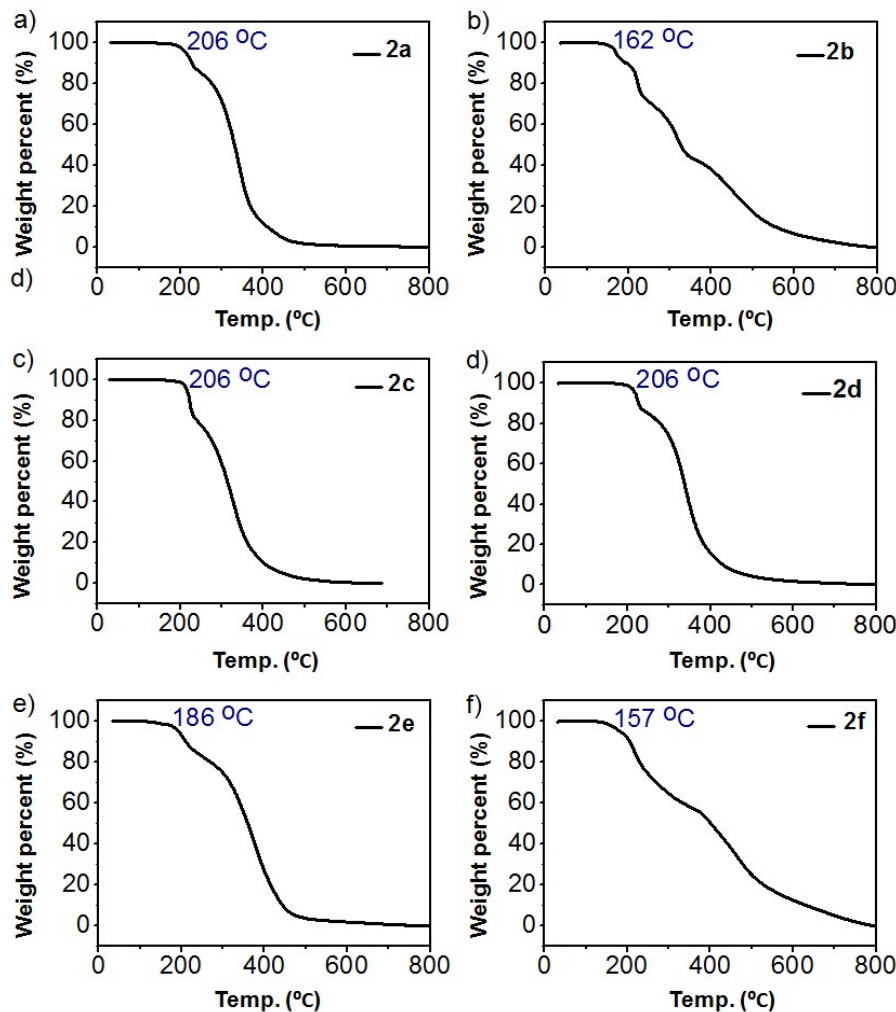


Figure S26. Measuring thermal stability of 2a-2f's solids. (a) ~ (f) Thermo gravimetric analysis (TGA) of 2a-2f.

For thermal stability, the starting decomposition temperatures for **2a**, **2b**, **2c**, **2d**, **2e** and **2f** were 206 °C, 162 °C, 206 °C, 206 °C, 186 °C and 157 °C, respectively. It indicates that these heterocycles have moderate thermal stability to resist high temperature. The results suggest that in these molecules, the coumarin group of the molecule has a weak thermal stability than the phenyl groups of the molecules (i.e., **2e** and **2f** vs. **2a**, **2b** and **2d**), and the nitro group on the indole subunit will relatively decrease the thermal stability of molecules (i.e., **2b** vs. **2a**, **2f** vs. **2e**).

21. HRMS spectra of **2b-OH** and UV-Vis spectra measurement for switch property of **2b**

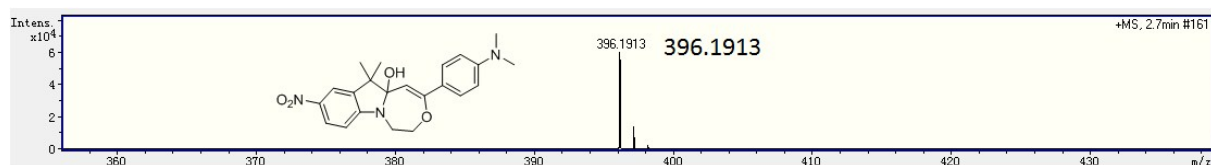


Figure S27. HRMS spectrum of **2b-OH** from the reaction of **2b** (4.0×10^{-4} M in DMSO) and aqueous solution of Na_2CO_3 .

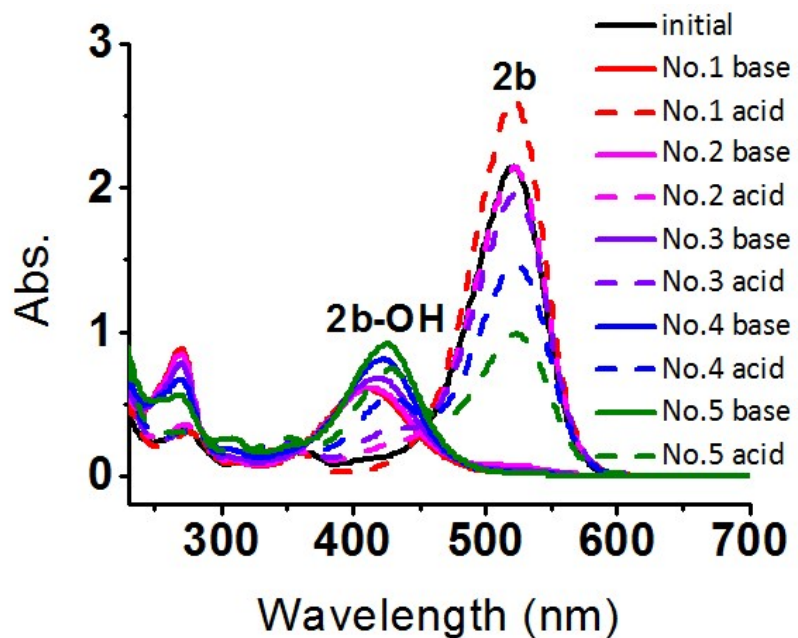


Figure S28. UV-Vis spectra of **2b** in DMSO (4.0×10^{-4} M) after repeated addition of aqueous solution of Na_2CO_3 and HCl.

22. Measurement of the pKa' of 2a-2f

The pKa'(s) of these heterocycles were tested by measuring the UV-Vis spectra of these heterocycles in buffers containing 1% DMSO with pH between 6 and 13. Although **2a-2f** are responsive to OH⁻, they are not really weak acid and with no dissociation equilibrium. Considering that they could react with OH⁻ and are Lewis acid, therefore we use pKa'(s) to evaluate their acidity and the ability to react with base.

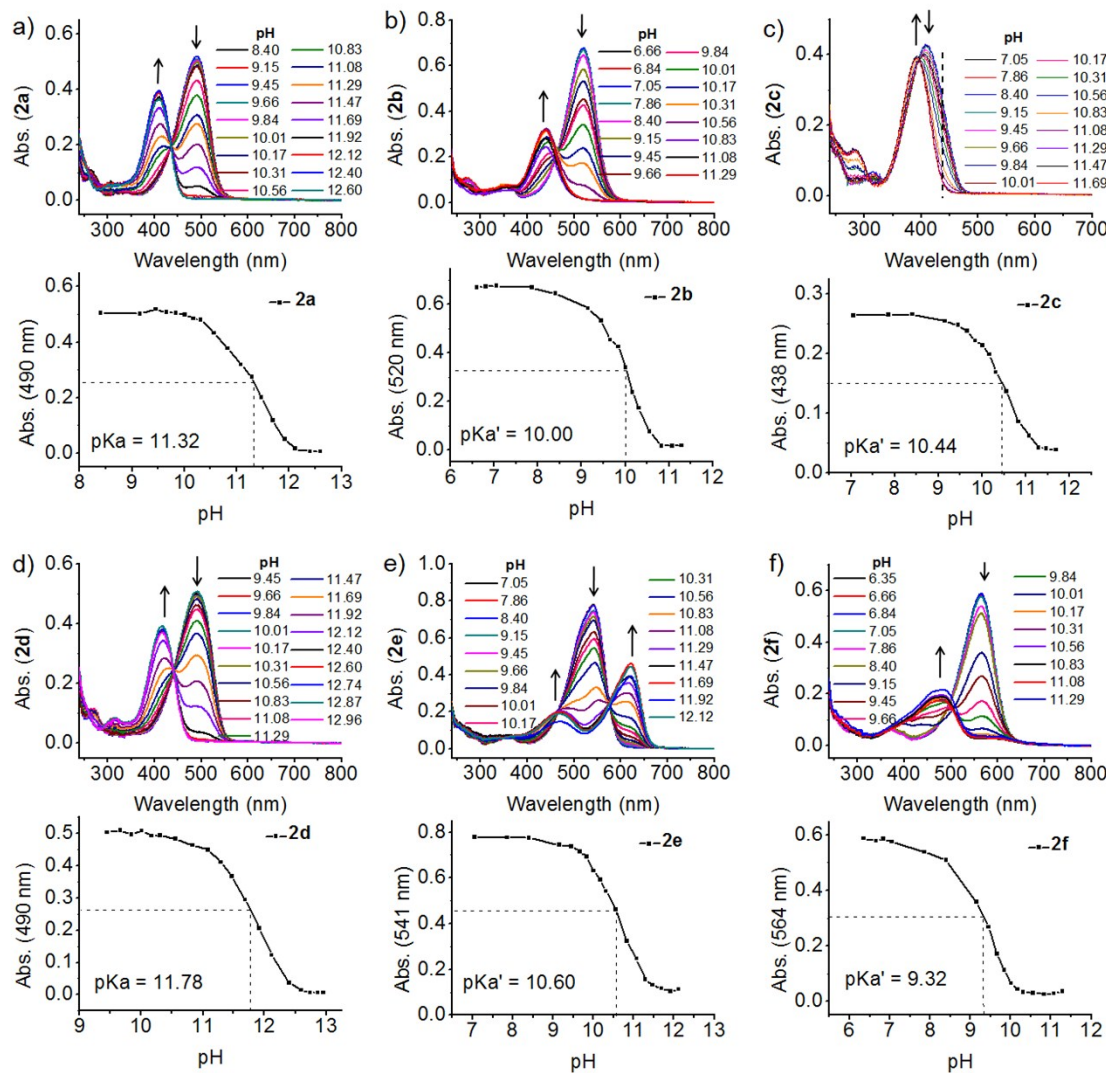


Figure S29. (a) ~ (f) UV-Vis absorption spectra of **2a-2f** in buffers with pH between 6.35 and 12.96 ($C = 1.0 \times 10^{-5}$ M) (above) and the intensity changes at its λ_{max} (**2a-2f**) with pH of buffers (below).

23. HRMS spectra monitoring reaction of 2b with amines

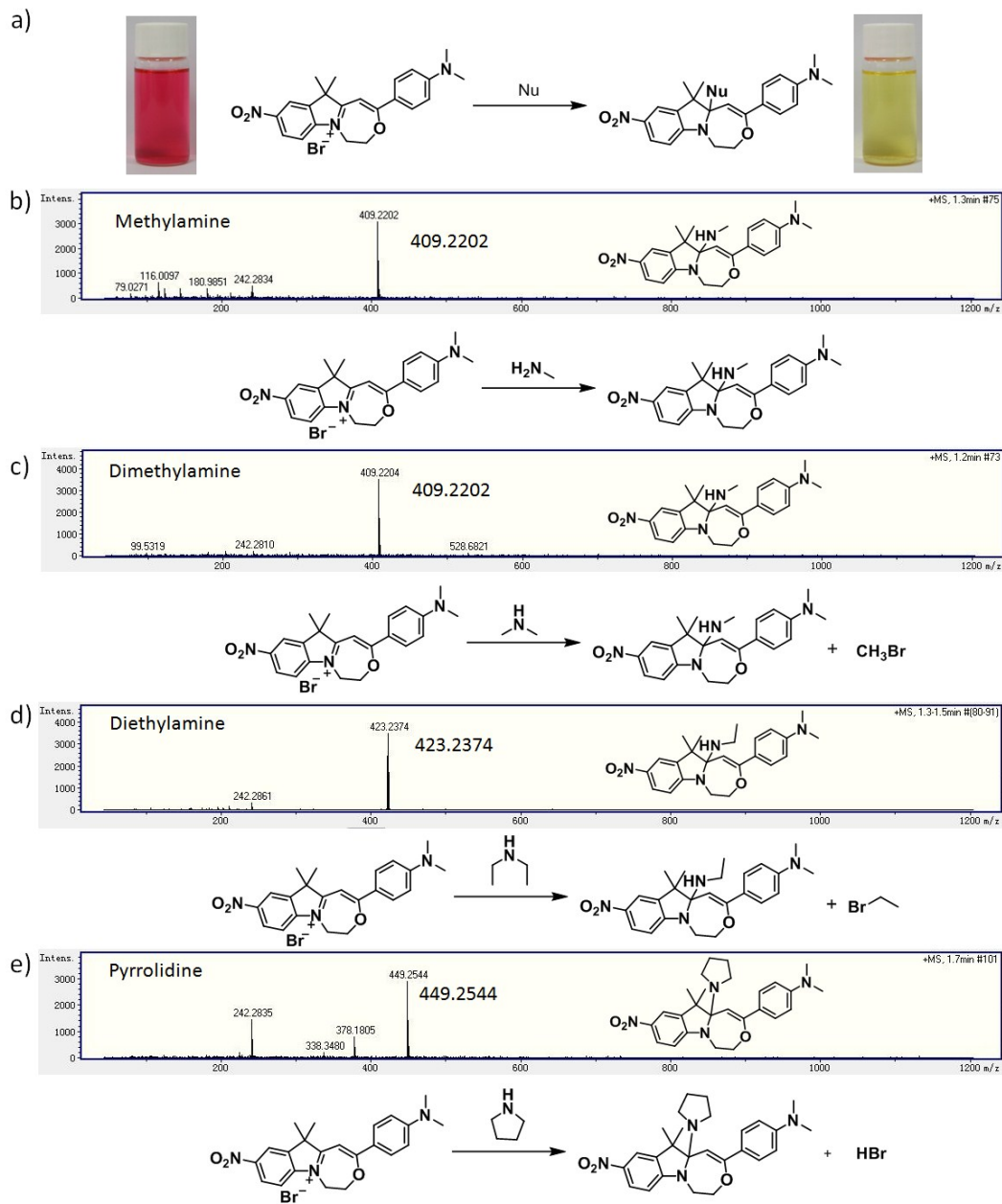


Figure S30. 2b in MeCN reacting with multiple nucleophilic reagents. (a) Photos and structural illustration of 2b reacting with nucleophilic reagents. HRMS spectra of 2b reacting with (b) methylamine, (c) dimethylamine, (d) diethylamine and (e) pyrrolidine.

24. The selectivity to pH of **2b over reactive nitrogen and oxygen species**

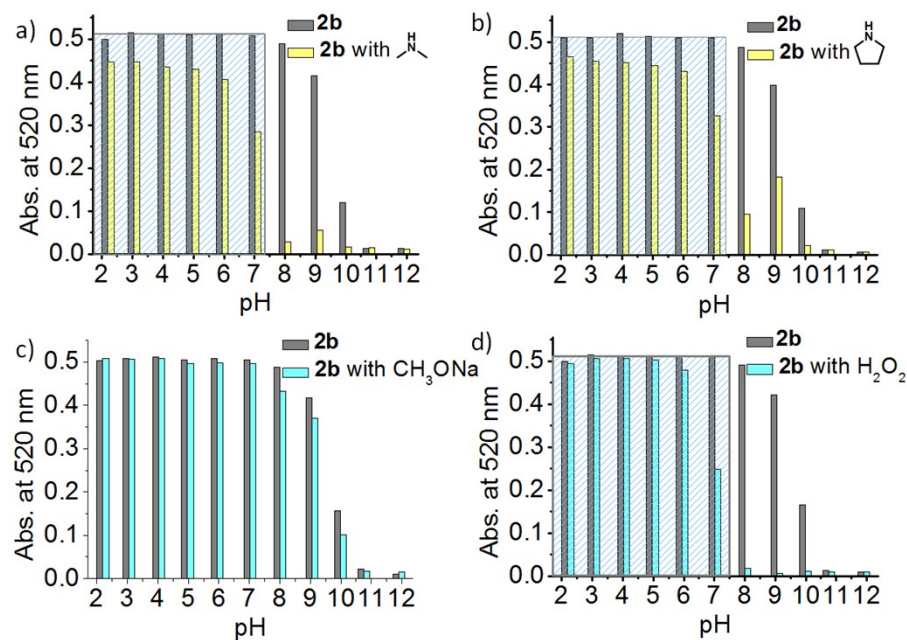


Figure S31. Effect of pH on the reaction of **2b** with nucleophilic reagents and hydrogen peroxide. The maximum absorption variation at 520 nm of **2b**'s buffer solutions (1.0×10^{-5} M) of different pH values before (grey bar) and after (light yellow or light cyan bar) adding (a) dimethylamine (1.45×10^{-4} M), (b) pyrrolidine (1.81×10^{-4} M), (c) sodium methoxide (2.44×10^{-4} M) and (d) hydrogen peroxide (1.50×10^{-4} M).

25. The cytotoxicity of 2e

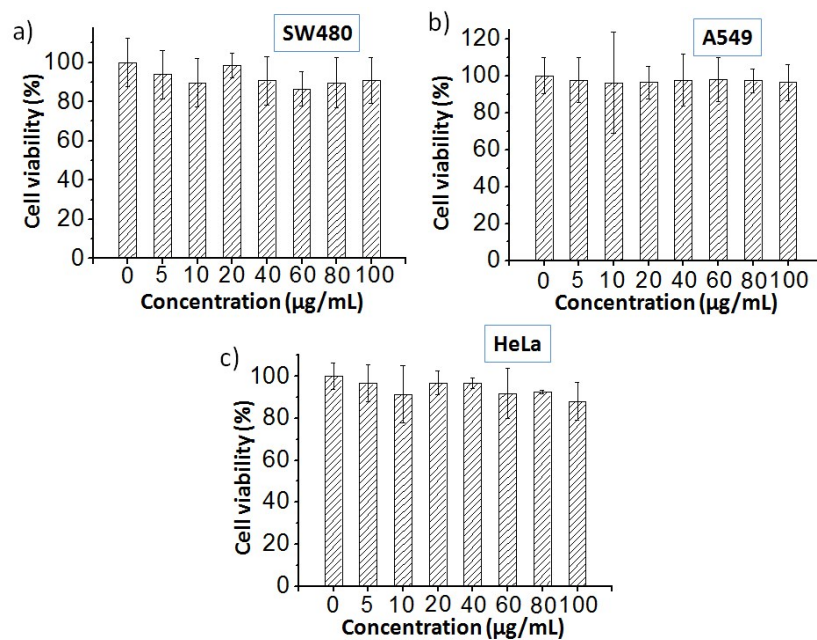


Figure S32. Effects of 2e at varied concentrations on the viability of (a) SW480, (b) A549 and (c) HeLa cells.

26. Effect of extracellular fluctuations under oxidative stress and with drug treatment on endocytosis efficiency and fluorescence of **2e**

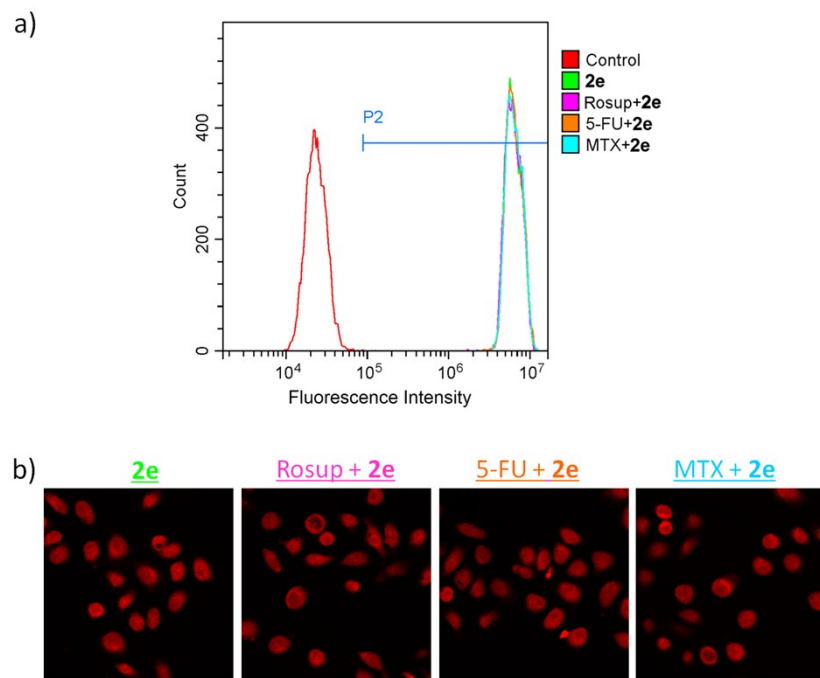


Figure S33. Measurement for effect of extracellular fluctuations of oxidative stress (Rosup) and drug treatment (5-fluorouracil (5-FU) and methotrexate (MTX)) on endocytosis efficiency of **2e** in HeLa cells by (a) flow cytometry and (b) CLSM.

27. ^1H NMR and ^{13}C NMR spectra

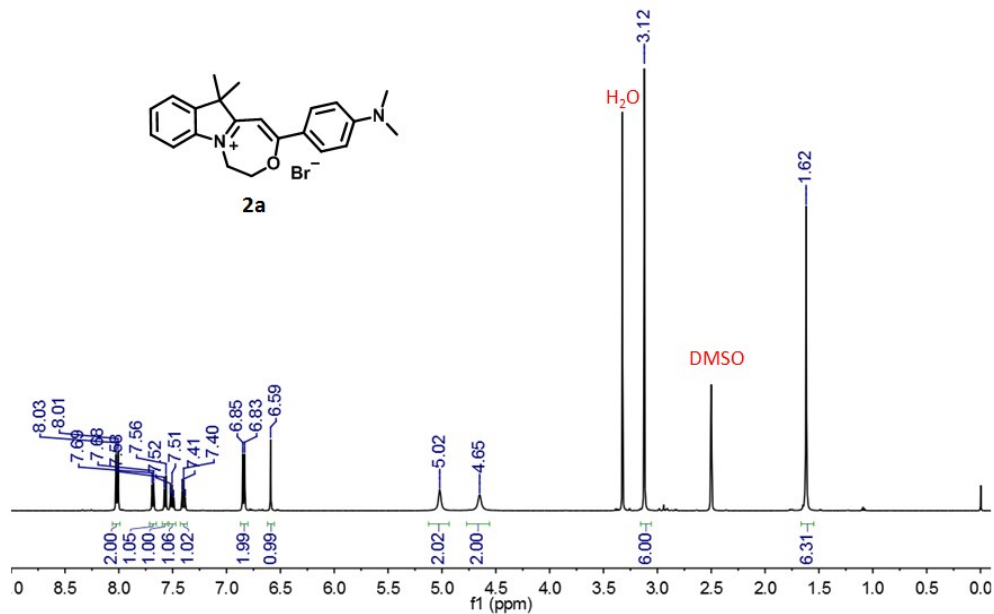


Figure S34. ^1H NMR spectrum of **2a** (400 MHz, $\text{DMSO}-d_6$).

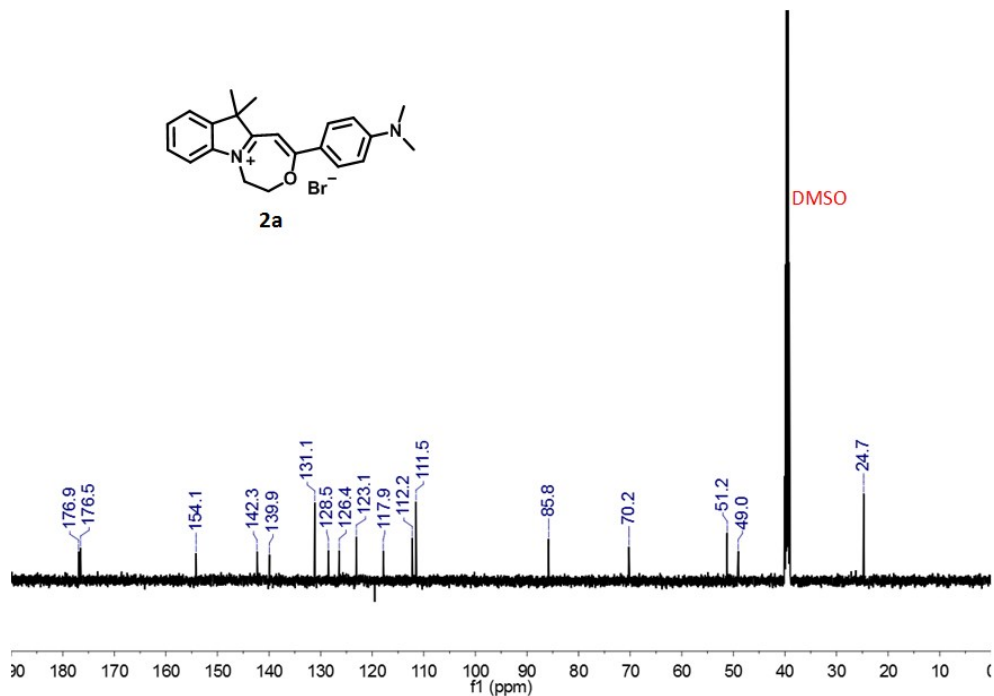


Figure S35. ^{13}C NMR spectrum of **2a** (125 MHz, $\text{DMSO}-d_6$).

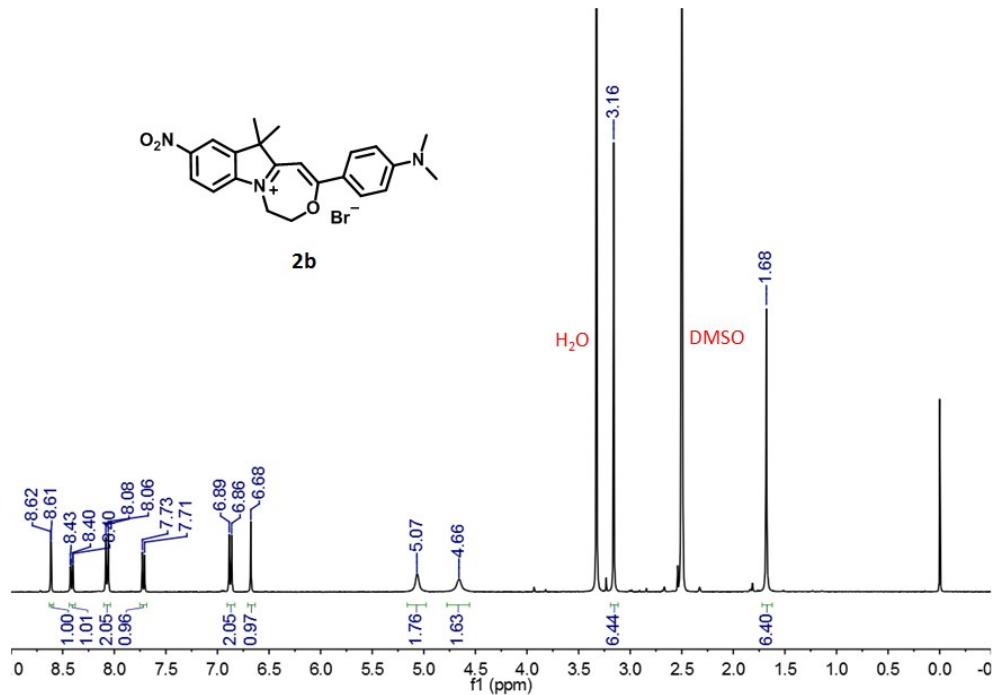


Figure S36. ^1H NMR spectrum of **2b** (400 MHz, $\text{DMSO}-d_6$).

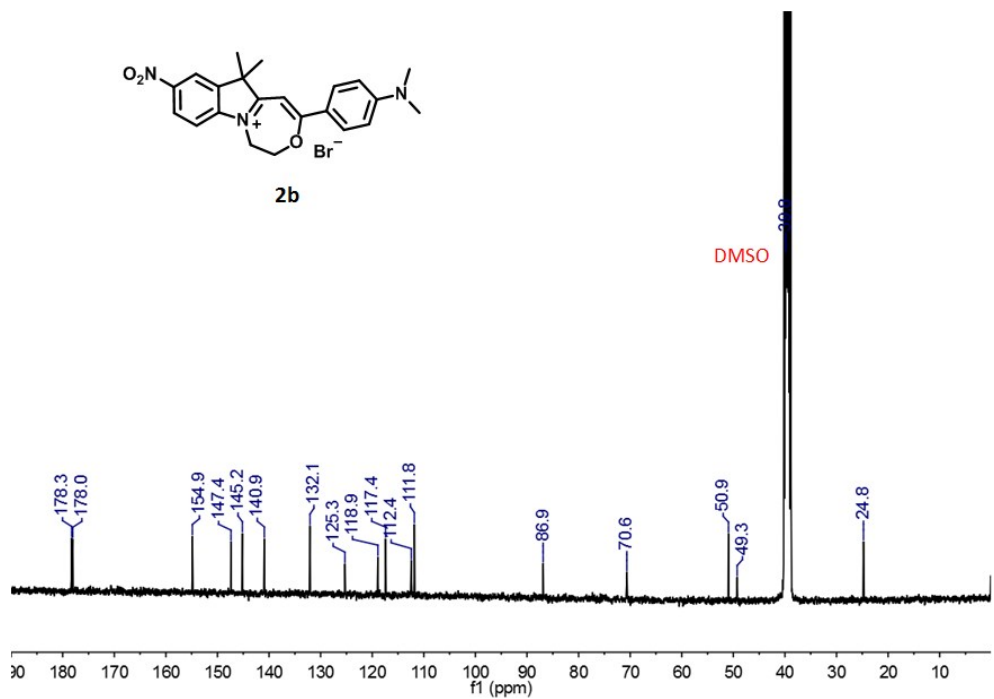


Figure S37. ^{13}C NMR spectrum of **2b** (100 MHz, $\text{DMSO}-d_6$).

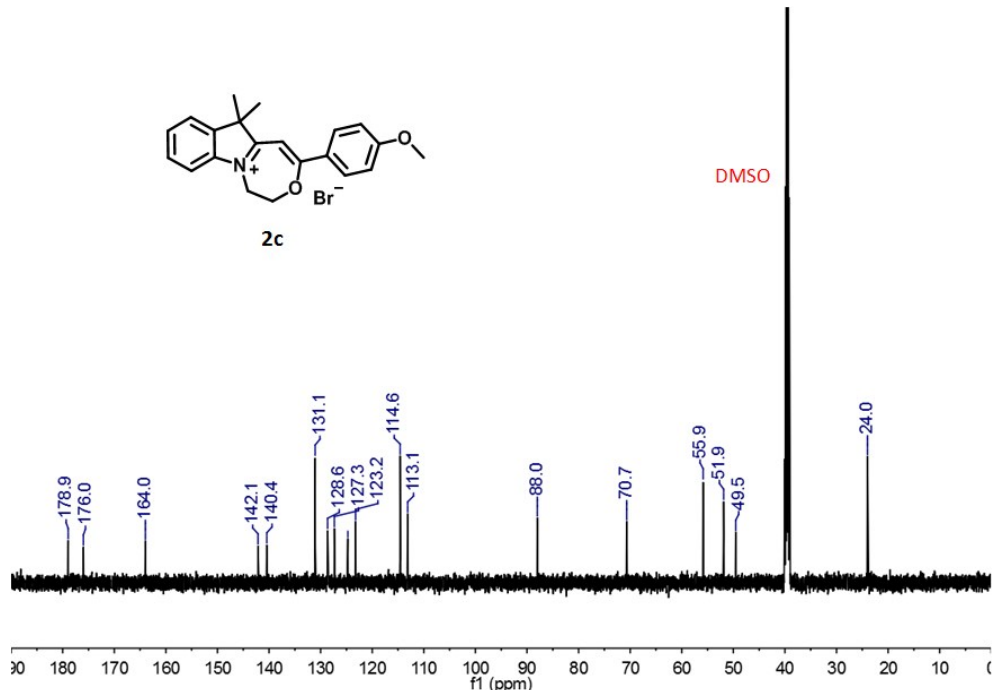
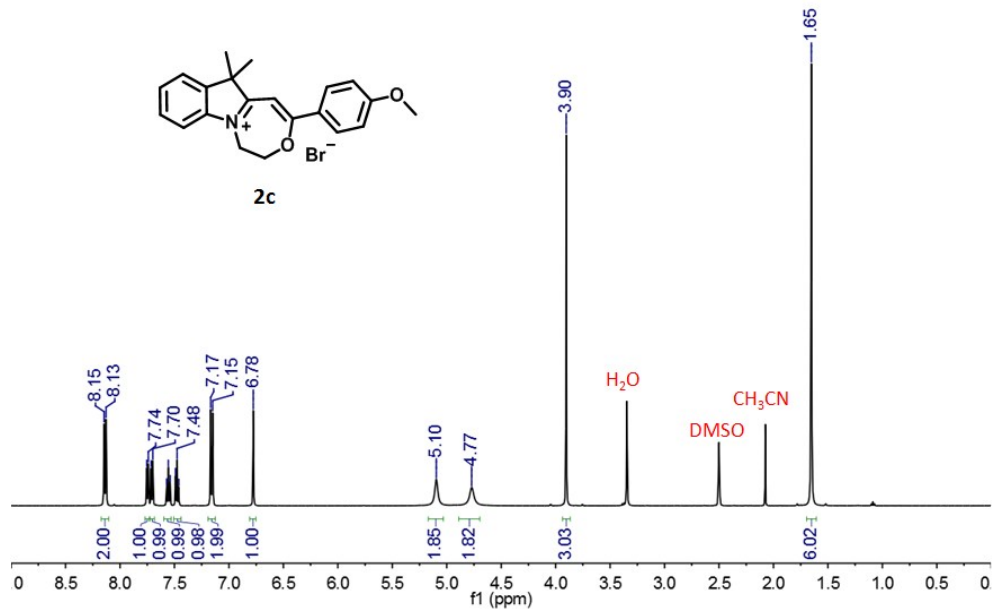


Figure S39. ^{13}C NMR spectrum of **2c** (100 MHz, $\text{DMSO}-d_6$).

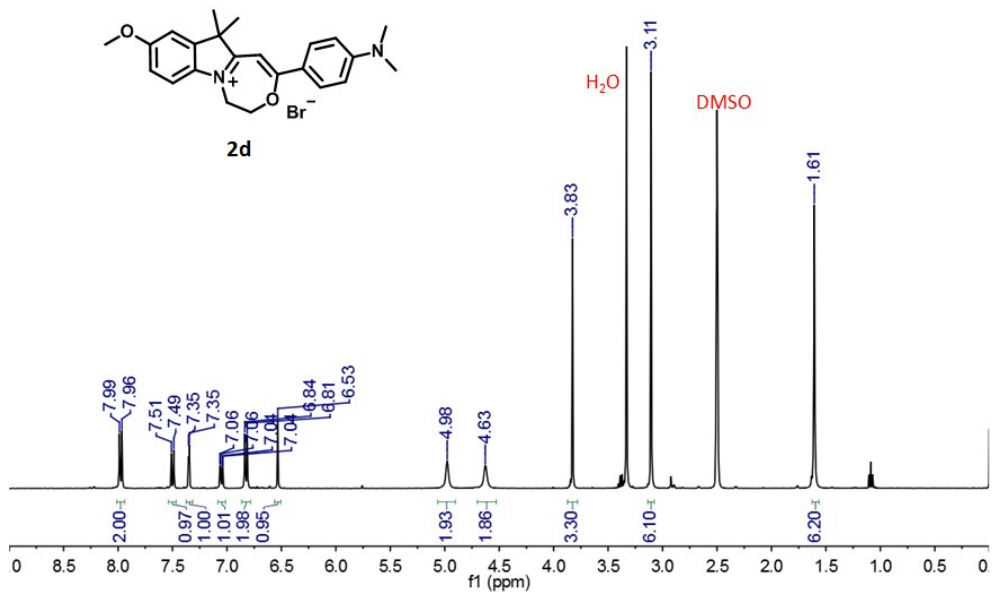


Figure S40. ^1H NMR spectrum of **2d** (400 MHz, DMSO- d_6).

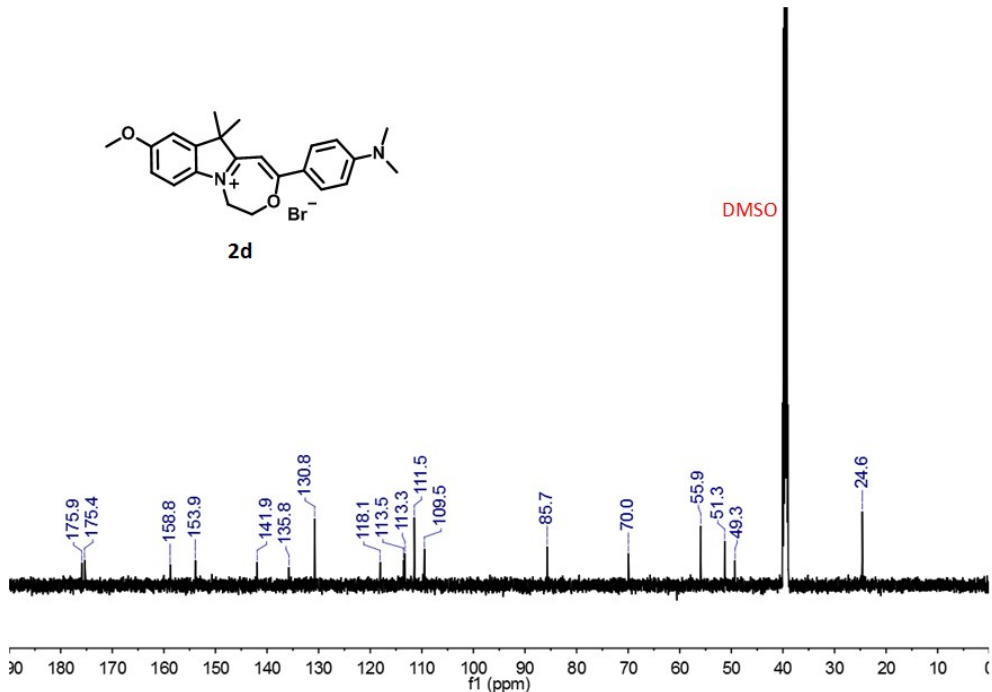


Figure S41. ^{13}C NMR spectrum of **2d** (126 MHz, $\text{DMSO-}d_6$).

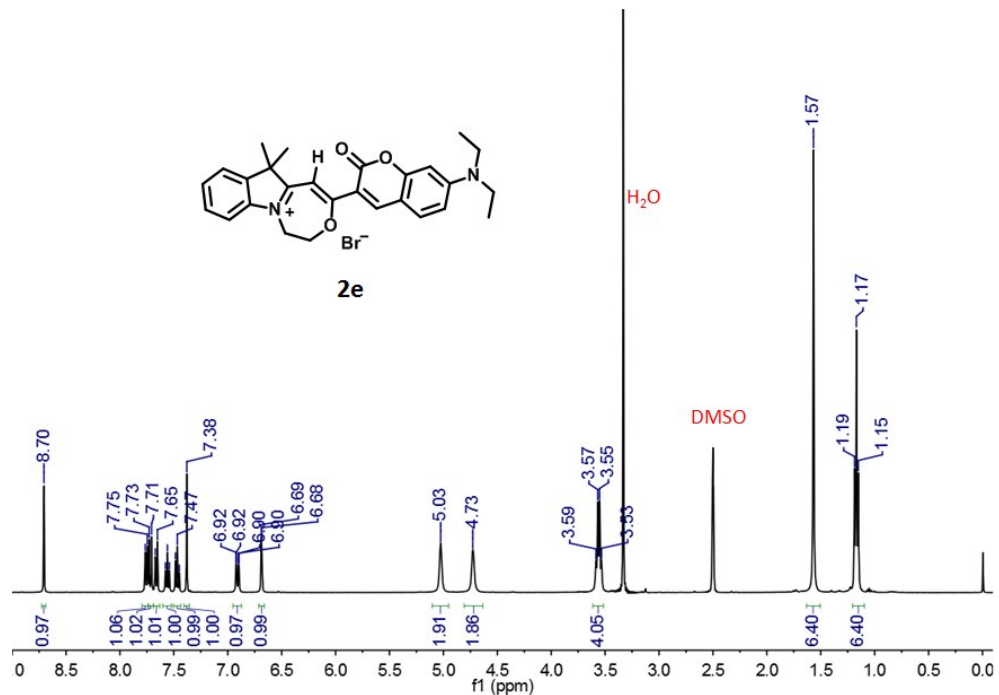


Figure S42. ¹H NMR spectrum of **2e** (400 MHz, $\text{DMSO}-d_6$).

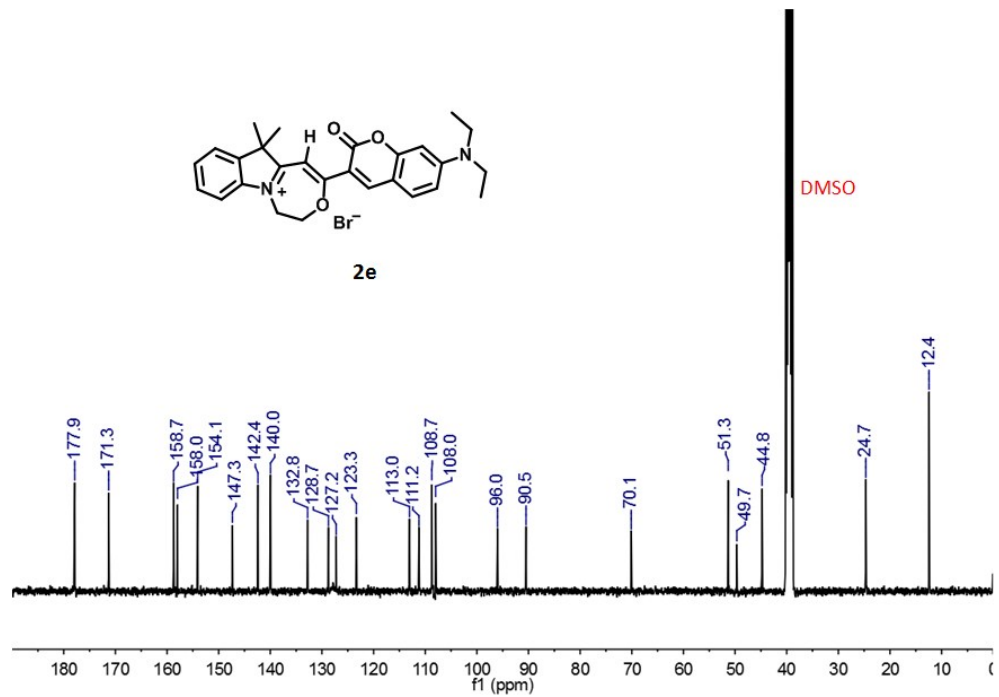


Figure S43. ¹³C NMR spectrum of **2e** (100 MHz, $\text{DMSO}-d_6$).

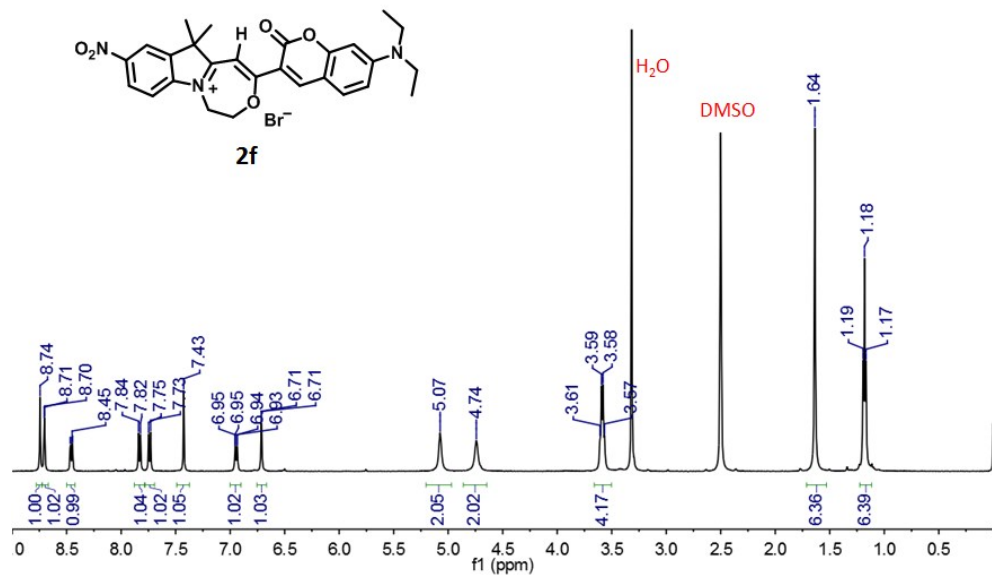


Figure S44. ^1H NMR spectrum of **2f** (400 MHz, $\text{DMSO}-d_6$).

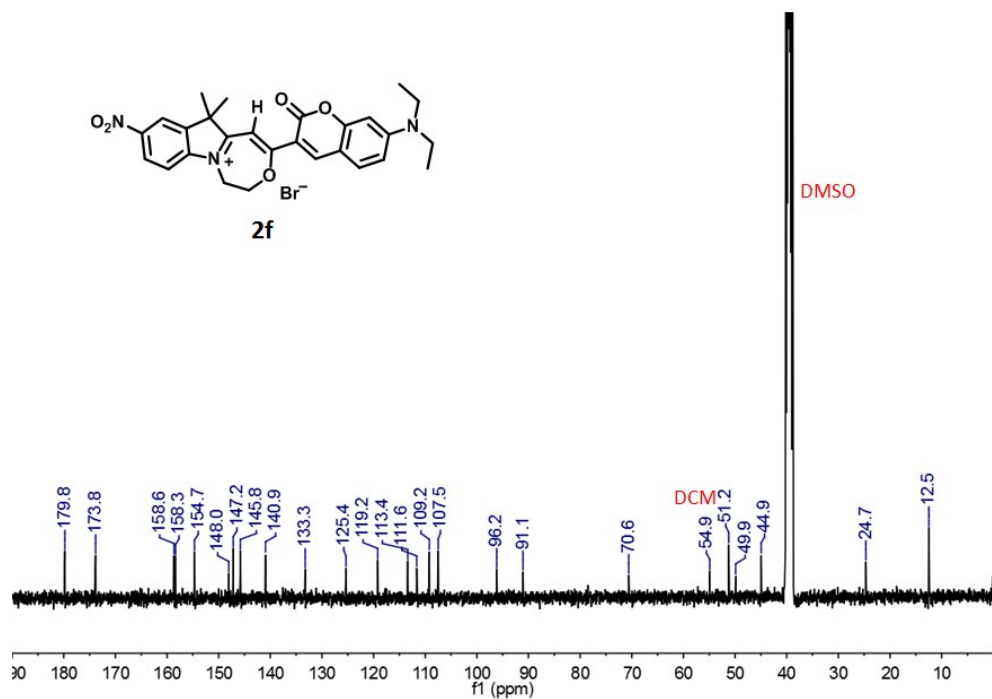


Figure S45. ^{13}C NMR spectrum of **2f** (100 MHz, $\text{DMSO}-d_6$).

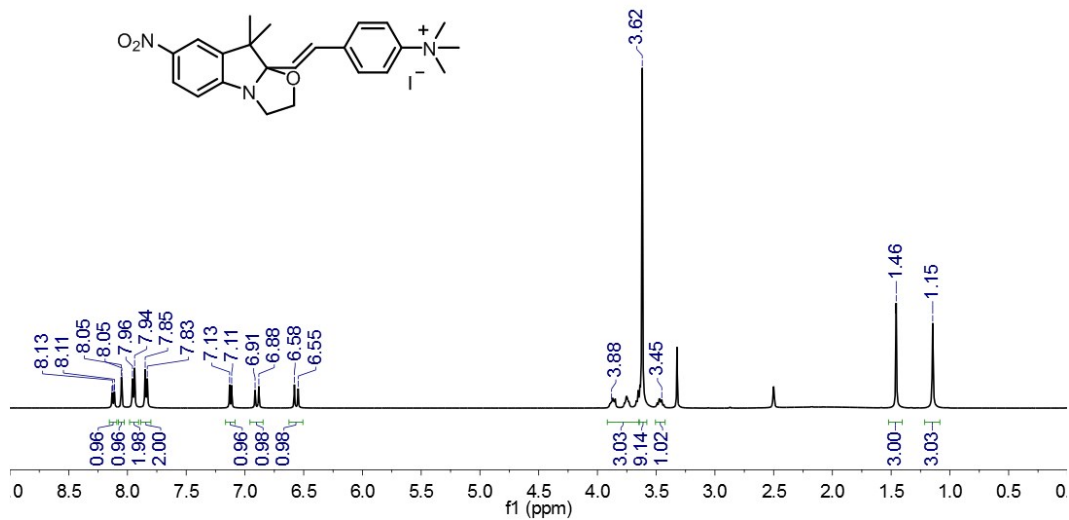


Figure S46. ^1H NMR spectrum of **I** (500 MHz, $\text{DMSO}-d_6$).

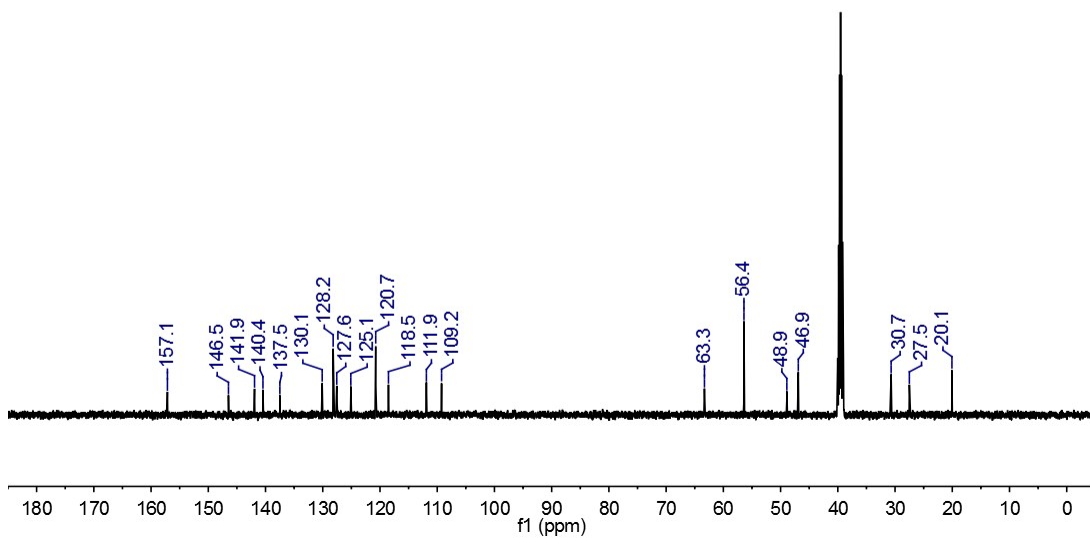


Figure S47. ^{13}C NMR spectrum of **I** (126 MHz, $\text{DMSO}-d_6$).

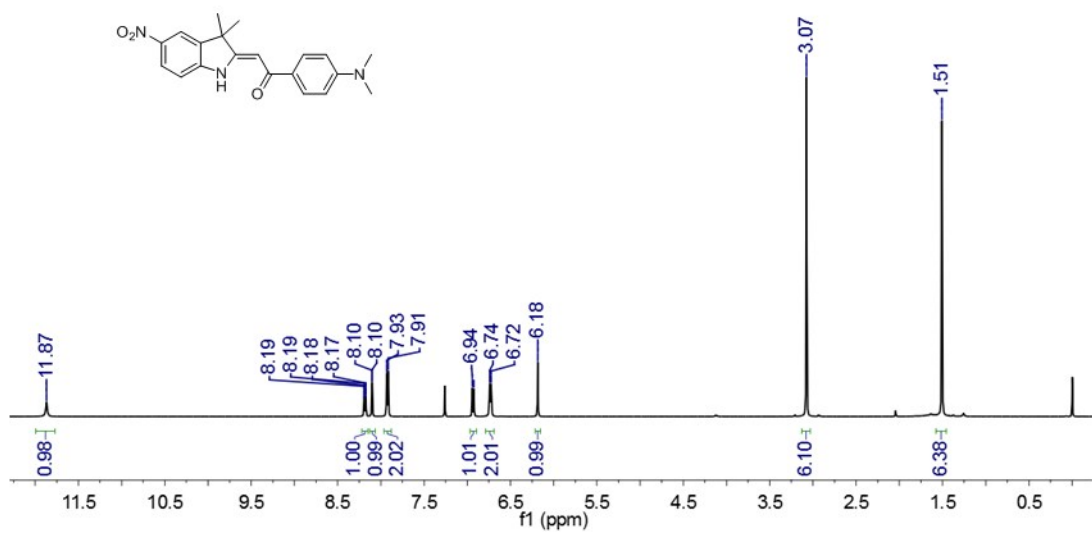


Figure S48. ^1H NMR spectrum of **3** (500 MHz, CDCl_3).

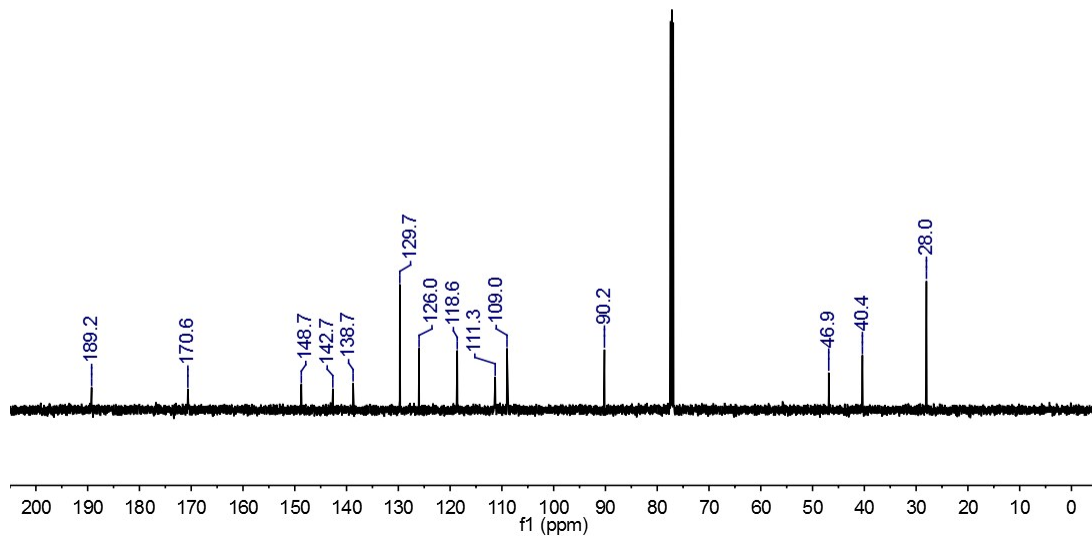
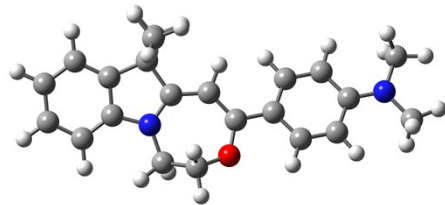


Figure S49. ^{13}C NMR spectrum of **3** (126 MHz, CDCl_3).

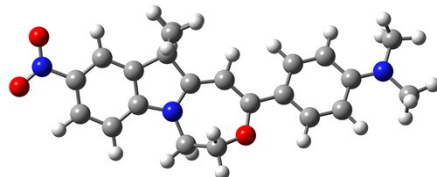
28. The coordination of structures



2a

C	3. 96644271	-0. 84461912	0. 02769471
C	5. 22420769	-1. 43131355	0. 00684497
H	5. 35183437	-2. 48964129	0. 21668254
C	6. 33617190	-0. 63301272	-0. 29176304
H	7. 32624972	-1. 07735822	-0. 31150529
C	6. 18311135	0. 72762128	-0. 57006790
H	7. 05397665	1. 33042151	-0. 80785382
C	4. 92041045	1. 33117088	-0. 55433545
H	4. 81360075	2. 38537008	-0. 78786729
C	3. 83604206	0. 51852484	-0. 24371694
C	2. 59547058	-1. 43342156	0. 30314615
C	2. 49183760	-1. 99825062	1. 74029233
H	2. 74996617	-1. 24178293	2. 48757711
H	3. 18424190	-2. 83829710	1. 85430058
H	1. 48096806	-2. 36309372	1. 94927842
C	2. 22886357	-2. 52178367	-0. 73389371
H	1. 22514359	-2. 92015410	-0. 55265215
H	2. 93733390	-3. 35228136	-0. 65677430
H	2. 27071316	-2. 13227941	-1. 75542108
C	1. 69466020	-0. 19821514	0. 14509035
C	0. 30806565	-0. 26717361	0. 28943225
H	-0. 05938517	-1. 26448837	0. 49180783
C	-0. 69169836	0. 70908749	0. 16242701
C	0. 80440199	2. 54729053	0. 59693041
H	0. 99915686	2. 18089257	1. 61088621
H	0. 65213571	3. 62720769	0. 63118663
C	1. 97182127	2. 23157856	-0. 33192523
H	1. 67470107	2. 39871244	-1. 37393758
H	2. 79510384	2. 91309819	-0. 10200920
C	-2. 09395956	0. 39723140	0. 07051516
C	-2. 56449119	-0. 90407767	-0. 23869201
H	-1. 86053463	-1. 70090971	-0. 45481533

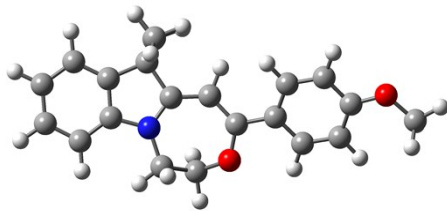
C	-3.90788790	-1.18920841	-0.32223528
H	-4.21073521	-2.19607004	-0.57933235
C	-4.89076269	-0.17892338	-0.10076368
C	-4.41907220	1.13382963	0.19475224
H	-5.12220030	1.93730658	0.37309776
C	-3.07212513	1.40479206	0.27125628
H	-2.75168075	2.41251892	0.50841069
C	-6.68015208	-1.81435936	-0.45670953
H	-6.36468762	-2.14597288	-1.45379285
H	-7.76885220	-1.83578907	-0.42040986
H	-6.30137235	-2.52538842	0.28674193
C	-7.20879735	0.60305846	0.02116927
H	-7.13958478	1.03525769	1.02676579
H	-8.20711648	0.18409749	-0.10039443
H	-7.08328407	1.40514325	-0.71576847
N	2.45970259	0.87097791	-0.15145533
N	-6.21931358	-0.45621467	-0.17274338
O	-0.44047234	2.02889745	0.12406241



2b

C	3.11371700	-0.52006735	0.10757308
C	4.39541715	-1.04143745	0.09912222
H	4.61269239	-2.08134806	0.31316309
C	5.44505016	-0.16798875	-0.20243758
C	5.24412747	1.17974380	-0.49456742
H	6.09939217	1.80157205	-0.72855490
C	3.95042553	1.70456478	-0.48710651
H	3.78923552	2.74923094	-0.72935551
C	2.90870206	0.83488694	-0.17456393
C	0.81173241	-0.00063216	0.20956723
C	1.77777818	-1.18362323	0.38206610
C	1.48003111	-2.29918248	-0.64848984
H	1.50330161	-1.91640721	-1.67323778
H	0.49956020	-2.75115386	-0.46679869
H	2.23344910	-3.08814958	-0.56144490

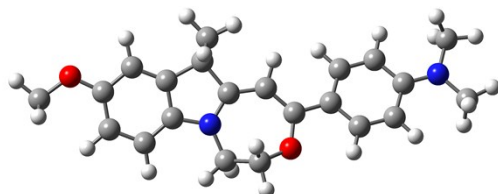
C	1. 70242328	-1. 74309022	1. 82343857
H	2. 43977813	-2. 54275389	1. 94586669
H	0. 71244077	-2. 16226609	2. 03009837
H	1. 91376538	-0. 96838604	2. 56680932
C	-0. 56476400	-0. 14297209	0. 34200042
H	-0. 87871167	-1. 15708964	0. 55075831
C	-1. 62041883	0. 77839250	0. 19658924
C	-0. 22856481	2. 69824241	0. 63523271
H	-0. 01953553	2. 34984444	1. 65262323
H	-0. 44151549	3. 76798799	0. 66151391
C	0. 95783778	2. 44213436	-0. 28773768
H	0. 65382028	2. 57965386	-1. 33210901
H	1. 73844084	3. 17379924	-0. 06331065
C	-2. 99645317	0. 38671936	0. 08313404
C	-4. 03475409	1. 34346005	0. 24010563
H	-3. 77615547	2. 37167958	0. 46429932
C	-5. 36099279	0. 99727375	0. 13737869
H	-6. 11127157	1. 76366357	0. 28321254
C	-5. 75303402	-0. 34621459	-0. 14332152
C	-4. 71019583	-1. 30635973	-0. 31820635
H	-4. 95137350	-2. 33345894	-0. 55989003
C	-3. 38818549	-0. 94639867	-0. 20855083
H	-2. 63749024	-1. 70831261	-0. 38995356
C	-8. 11204116	0. 31053866	-0. 09652525
H	-8. 09492746	0. 76110577	0. 90303611
H	-9. 08166126	-0. 16517333	-0. 23888062
H	-8. 00835216	1. 10549712	-0. 84412454
C	-7. 43976396	-2. 08391174	-0. 51114302
H	-7. 07430759	-2. 41770960	-1. 48993131
H	-8. 52635890	-2. 16194987	-0. 50907060
H	-7. 04865043	-2. 75685463	0. 26053543
N	6. 82059022	-0. 69935721	-0. 21699182
N	1. 52270553	1. 11278954	-0. 09091593
N	-7. 05976521	-0. 69618148	-0. 24416695
O	6. 96396455	-1. 89228472	0. 04277273
O	7. 72672117	0. 08425271	-0. 48658586
O	-1. 44052602	2. 10825126	0. 15855322



2c

C	-3.67922024	-0.77148786	0.03262510
C	-4.96159897	-1.30308027	0.02023044
H	-5.13242352	-2.35878543	0.21089876
C	-6.04115643	-0.45061069	-0.24474613
H	-7.04996448	-0.85082215	-0.25747409
C	-5.83381060	0.90807319	-0.49867841
H	-6.68142968	1.55216233	-0.71034463
C	-4.54640432	1.45629181	-0.49138922
H	-4.39746998	2.50940700	-0.70566562
C	-3.49525474	0.58996539	-0.21424623
C	-1.38313992	-0.22442771	0.12718142
C	-2.33084255	-1.42297785	0.27373975
C	-2.02412884	-2.50297187	-0.79221674
H	-2.76584384	-3.30416382	-0.72045004
H	-1.03598687	-2.94694899	-0.63409795
H	-2.06506681	-2.09078236	-1.80479765
C	-2.22639014	-2.02210094	1.69759631
H	-2.44222743	-1.27272118	2.46510828
H	-1.22825761	-2.43238376	1.88142470
H	-2.95037402	-2.83588847	1.80429783
C	-1.55150434	2.21798027	-0.30938660
H	-2.34337946	2.93455969	-0.07755543
H	-1.24625432	2.37474989	-1.35028135
C	-0.37242221	2.47503509	0.62391464
H	-0.17451196	3.54679158	0.67096907
H	-0.58196914	2.10395446	1.63311159
C	1.03768706	0.58339742	0.13904621
C	0.00722383	-0.35339088	0.24634674
H	0.33778430	-1.37099283	0.40701699
C	2.43467332	0.20913583	0.02104116
C	2.82971270	-1.08597360	-0.39851852
H	2.08400935	-1.82179897	-0.68001180
C	4.16137129	-1.42290254	-0.50423322
H	4.47001946	-2.40790665	-0.83740110
C	5.16215478	-0.47554017	-0.19609758

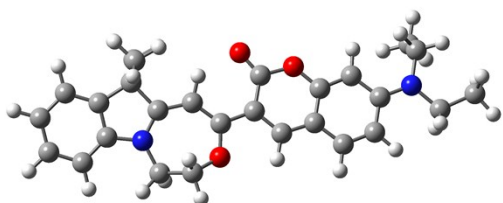
C	4. 79025906	0. 81940063	0. 21201712
H	5. 54018131	1. 56213705	0. 45555487
C	3. 44774892	1. 14883202	0. 31111462
H	3. 17144235	2. 14576666	0. 63405364
C	7. 50874766	-0. 01017972	-0. 05433174
H	7. 48001397	0. 85645969	-0. 72383656
H	8. 41435266	-0. 58712556	-0. 23941067
H	7. 48913487	0. 32013979	0. 99001855
N	-2. 10107907	0. 87883481	-0. 13815855
O	0. 85208639	1. 91056355	0. 14720237
O	6. 42460641	-0. 90462066	-0. 32846140



2d

C	3. 31016555	-0. 67652687	0. 11773626
C	4. 57302173	-1. 23327197	0. 12677856
H	4. 74863980	-2. 28175517	0. 34608019
C	5. 68350659	-0. 41098221	-0. 16016731
C	5. 49842134	0. 94885825	-0. 45691137
H	6. 34576075	1. 58258382	-0. 68758828
C	4. 21544617	1. 50933887	-0. 46720309
H	4. 09321584	2. 55900835	-0. 71402023
C	3. 14270347	0. 68214558	-0. 16922075
C	1. 95079954	-1. 30163401	0. 37526670
C	1. 83993522	-1. 85741033	1. 81482582
H	2. 06358680	-1. 08754121	2. 55955068
H	2. 55467499	-2. 67573690	1. 94730456
H	0. 83660258	-2. 24938201	2. 01045607
C	1. 63335631	-2. 40736826	-0. 65900931
H	0. 63836096	-2. 83258872	-0. 49155188
H	2. 36429894	-3. 21624165	-0. 56391022
H	1. 68121873	-2. 02393028	-1. 68258772
C	1. 01770361	-0. 09320818	0. 19115769
C	-0. 37091244	-0. 20105500	0. 31496020
H	-0. 71183408	-1. 20726675	0. 52019099
C	-1. 39454624	0. 74276010	0. 16484668
C	0. 03963273	2. 62883042	0. 59871519

H	0.22851738	2.27972000	1.61996346
H	-0.14285989	3.70451650	0.61806066
C	1.23165905	2.33650508	-0.30680488
H	0.94761028	2.48321137	-1.35543997
H	2.03181132	3.04334669	-0.07095273
C	-2.78828554	0.39069316	0.06066682
C	-3.21839317	-0.92382205	-0.24782648
H	-2.48969888	-1.70070792	-0.45470667
C	-4.55287061	-1.24785007	-0.34265925
H	-4.82401245	-2.26400391	-0.59884677
C	-5.56589789	-0.26568451	-0.13486973
C	-5.13457121	1.06028032	0.15996163
H	-5.86156171	1.84441960	0.32849824
C	-3.79601684	1.37003798	0.24822551
H	-3.50691719	2.38748819	0.48434269
C	-7.30470014	-1.95233469	-0.50282308
H	-6.96838006	-2.27939797	-1.49473458
H	-8.39276620	-2.00503637	-0.47901829
H	-6.91461698	-2.64981701	0.24777121
C	-7.90660868	0.45066885	-0.04103778
H	-7.86103620	0.88911416	0.96337013
H	-8.89164731	0.00375887	-0.17184028
H	-7.79553607	1.25351127	-0.77968956
N	1.75526979	0.99266401	-0.10369135
N	-6.88637209	-0.58098958	-0.21947826
O	-1.18123568	2.07035403	0.11180860
O	6.88370085	-1.03485598	-0.12691664
C	8.06280534	-0.28169740	-0.40273380
H	8.88978968	-0.98592442	-0.30940246
H	8.04428663	0.12703993	-1.42031662
H	8.19236365	0.53226785	0.32082361

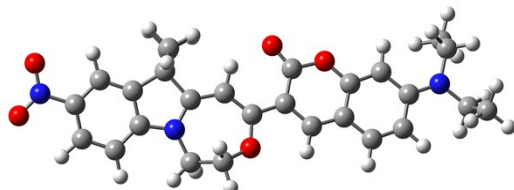


2e

C	5.74676316	-0.76340985	-0.04014029
C	7.01893199	-1.31586550	-0.09754536

H	7.18327085	-2.36565030	0.12833452
C	8.09583648	-0.49416242	-0.45490936
C	7.89560634	0.85595237	-0.75544835
H	8.74036167	1.47621102	-1.03824428
C	6.61850600	1.42557181	-0.70404211
H	6.47347858	2.47141656	-0.95405072
C	5.57001828	0.59020149	-0.33522597
C	3.46853273	-0.17267493	0.15840484
C	4.40314348	-1.38103160	0.29530993
C	4.01358123	-2.48435890	-0.72058895
H	4.02998644	-2.10536399	-1.74691290
H	3.01496116	-2.87938627	-0.51051279
H	4.72913173	-3.30948172	-0.65048449
C	4.36284520	-1.93950490	1.73823314
H	5.07717116	-2.76374463	1.83022252
H	3.36795861	-2.32526234	1.98094940
H	4.63079665	-1.17386299	2.47286552
C	2.08858370	-0.28920179	0.35788366
H	1.74389137	-1.29510907	0.55129872
C	1.05683033	0.64045594	0.24028684
C	2.48962970	2.55317817	0.52769326
H	2.71918758	2.24029989	1.55236192
H	2.29896403	3.62766919	0.51830668
C	3.65229312	2.24445814	-0.40902891
H	3.33494448	2.36580489	-1.45123213
H	4.45545790	2.96042891	-0.21427960
N	4.18868150	0.90718476	-0.19585607
O	1.25568739	1.96930610	0.10814378
C	-0.34683062	0.29145211	0.23566482
C	-1.31600576	1.29359970	0.21425082
C	-0.78301827	-1.11484696	0.22851856
C	-2.68535507	1.01119376	0.17190476
H	-0.99574852	2.33000621	0.22918362
C	-3.09090690	-0.34828076	0.15122077
C	-3.71695887	1.98719670	0.13704236
C	-4.41283580	-0.73269593	0.10279924
C	-5.03910567	1.63206539	0.08964396
H	-3.44313315	3.03874135	0.14266626
C	-5.44272390	0.24931844	0.08352780
H	-4.62289752	-1.79222307	0.07464597
H	-5.78266789	2.41535479	0.05270849
O	-0.08910152	-2.10738192	0.26491427
O	-2.15397252	-1.33609520	0.17689148
N	-6.75946628	-0.09499363	0.06448241
C	-7.78425131	0.97201826	-0.03682638

H	-7.60012631	1.69091608	0.76912254
H	-7.64284536	1.50811445	-0.98518379
C	-7.16128808	-1.50742799	-0.03382947
H	-6.51920341	-2.09548580	0.62702325
H	-8.16515362	-1.59755426	0.37883048
H	9.09647939	-0.91197115	-0.50337011
C	-7.13046827	-2.06042193	-1.46331059
H	-6.12961756	-1.99388811	-1.90133270
H	-7.43286613	-3.11311966	-1.46119243
H	-7.82005930	-1.51162759	-2.11317721
C	-9.23679936	0.51397583	0.06418139
H	-9.45858310	0.04322104	1.02689017
H	-9.87127240	1.40211905	-0.01914733
H	-9.52460415	-0.16906993	-0.74029248



2f

C	4.87495500	-0.48698432	0.11121404
C	6.16228806	-0.99511698	0.09972223
H	6.39475531	-2.02115185	0.35941511
C	7.19525920	-0.12714873	-0.26758660
C	6.97432717	1.20270880	-0.62174367
H	7.81807145	1.81989741	-0.90432380
C	5.67576467	1.71464180	-0.61161097
H	5.49787348	2.74470555	-0.90027455
C	4.65100879	0.85087500	-0.23336455
C	2.57428867	0.01862208	0.24609978
C	3.55147162	-1.14745011	0.44305708
C	3.22865843	-2.30015450	-0.54115836
H	3.25033450	-1.95690057	-1.57987593
H	2.24194970	-2.72580859	-0.33555789
H	3.97373539	-3.09370162	-0.42788216
C	3.50798498	-1.65749231	1.90397709
H	4.25377312	-2.44726259	2.03774975
H	2.52521282	-2.07646991	2.14019360
H	3.72787465	-0.85667223	2.61667360
C	1.20148745	-0.14328545	0.41816698

H	0. 89051434	-1. 15467677	0. 63848379
C	0. 13251239	0. 74279383	0. 24255965
C	1. 48707327	2. 71687906	0. 50682390
H	1. 70801352	2. 44333745	1. 54442397
H	1. 25462637	3. 78207183	0. 46157828
C	2. 67743807	2. 42627842	-0. 40042958
H	2. 37280327	2. 49829099	-1. 45102014
H	3. 44582060	3. 18240030	-0. 21776999
N	8. 57643531	-0. 64415639	-0. 28569815
N	3. 26381937	1. 11951756	-0. 13102921
O	8. 74004702	-1. 82029977	0. 03158405
O	9. 46754191	0. 13415690	-0. 61520199
O	0. 28441692	2. 07292449	0. 08140866
C	-1. 24915882	0. 33446073	0. 20413803
C	-2. 26172970	1. 29546835	0. 12701476
C	-1. 62546763	-1. 08905921	0. 21961979
C	-3. 61202284	0. 95389616	0. 04829102
H	-1. 98591175	2. 34464322	0. 12633438
C	-3. 96017394	-0. 42403074	0. 05143416
C	-4. 68322420	1. 88720756	-0. 03778415
C	-5. 26217654	-0. 86372694	-0. 02923663
C	-5. 98504279	1. 47658079	-0. 11967725
H	-4. 45291078	2. 94902950	-0. 03219829
C	-6. 32741078	0. 07625877	-0. 12000671
H	-5. 43420261	-1. 93079339	-0. 04255316
H	-6. 76503910	2. 22438436	-0. 16235238
O	-0. 89343833	-2. 05022876	0. 30191973
O	-2. 98476364	-1. 36917865	0. 13202666
N	-7. 61860735	-0. 32786079	-0. 20011394
C	-8. 73301627	0. 61401163	-0. 40412527
H	-9. 50845287	0. 06783163	-0. 94967967
H	-8. 40831824	1. 41795290	-1. 06941461
C	-8. 00240553	-1. 74601848	-0. 09259240
H	-7. 35419076	-2. 23681517	0. 63805825
H	-9. 00966849	-1. 76750816	0. 33418327
C	-9. 30511101	1. 17236241	0. 90239879
H	-8. 55439180	1. 74306151	1. 45813808
H	-10. 14982395	1. 83482589	0. 68618087
H	-9. 66541997	0. 36737674	1. 55149719
C	-7. 98376283	-2. 48467117	-1. 43456008
H	-6. 98135628	-2. 49599115	-1. 87372721
H	-8. 30759327	-3. 52106248	-1. 29297055
H	-8. 66293055	-2. 01392978	-2. 15316402

29. References

- S1 Q. Chen, L. Sheng, J. Du, G. Xi, S. X.-A. Zhang, *Chem. Commun.* 2018, **54**, 5094-5097.
- S2 Gaussian 09, Revision D.01, M. J. Frisch, G. W. Trucks, H. B. Schlegel, G. E. Scuseria, M. A. Robb, J. R. Cheeseman, G. Scalmani, V. Barone, B. Mennucci, G. A. Petersson, H. Nakatsuji, M. Caricato, X. Li, H. P. Hratchian, A. F. Izmaylov, J. Bloino, G. Zheng, J. L. Sonnenberg, M. Hada, M. Ehara, K. Toyota, R. Fukuda, J. Hasegawa, M. Ishida, T. Nakajima, Y. Honda, O. Kitao, H. Nakai, T. Vreven, J. A. Montgomery, Jr., J. E. Peralta, F. Ogliaro, M. Bearpark, J. J. Heyd, E. Brothers, K. N. Kudin, V. N. Staroverov, T. Keith, R. Kobayashi, J. Normand, K. Raghavachari, A. Rendell, J. C. Burant, S. S. Iyengar, J. Tomasi, M. Cossi, N. Rega, J. M. Millam, M. Klene, J. E. Knox, J. B. Cross, V. Bakken, C. Adamo, J. Jaramillo, R. Gomperts, R. E. Stratmann, O. Yazyev, A. J. Austin, R. Cammi, C. Pomelli, J. W. Ochterski, R. L. Martin, K. Morokuma, V. G. Zakrzewski, G. A. Voth, P. Salvador, J. J. Dannenberg, S. Dapprich, A. D. Daniels, O. Farkas, J. B. Foresman, J. V. Ortiz, J. Cioslowski, and D. J. Fox, Gaussian, Inc., Wallingford CT, **2013**